QUANTITATIVE TECHNIQUES IN RADIOISOTOPE IMAGING

by

Sirithorn Asavavekinkul

A thesis submitted for the degree of Master of Science in the Faculty of Science, University of Glasgow, from research conducted in the Department of Nuclear Medicine, Royal Infirmary, Glasgow.

July 1976.

TABLE OF CONTENTS

LIST OF TABLES

LIST OF ILLUSTRATIONS

LIST OF APPENDICES

ACKNOWLEDGEMENTS

This work was supported by a grant from the World Health Organisation.

I should like to thank Professor J.M.A. Lenihan of the Department of Clinical Physics and Bio-Engineering and Dr. W.R. Greig of the Department of Nuclear Medicine, Glasgow Royal Infirmary, for providing facilities to conduct this work, Dr. F.C. Gillespie, Dr. J. Shimmins and Dr. I.R. McDougall for their valuable advice, and also all the staff of the Department of Nuclear Medicine, Glasgow Royal Infirmary, for their help.

My special thanks go to Dr. R.G. Bessent, Principal Physicist, for his valuable guidance and encouragement throughout the time in the Department.

Miss Joyce Muir is to be thanked for typing the thesis and Mrs. Brenda Burn and her staff in the Department of Medical Illustration for excellent art work.

SUMMARY

The items of equipment comprising a radioisotope imaging system are briefly described, namely the Ohio-Nuclear R100 gamma camera, the Varian 620/L-100 minicomputer, the interface and the colour T.V. display, together with the relevant software.

The performance of the imaging system was analysed by line spread functions using ^{99m}Tc from which the Full Width at Half Maximum (FWHM) and the Modulation Transfer Functions (M.T.F.) were calculated. In this way spatial frequency response was determined at different distances from the "High Resolution" and "Ultra High Resolution" collimators in air.

The effect on overall spatial resolution of the number of computer memory locations used for image storage was investigated by adjusting the gain of the A.D.C. in the X direction to 1, 2, 4 and 16 times normal gain and the M.T.F.'s were calculated. The calculation of the M.T.F. was done by using a program written in BASIC.

A study was carried out of the application of the minicomputer interfaced to the gamma camera in improving diagnosis

for static images. The simple methods of image processing, namely smoothing and spatial frequency filtering, were used. Smoothing was done on a 3 x 3 matrix (nine point smoothing) by the smoothing function

$$\begin{bmatrix} 1 & 1 & 1 \\ 1 & 1 & 1 \\ 1 & 1 & 1 \end{bmatrix}$$

suggested by Nakamura et al (1973). Spatial frequency filtering was done on a 5 x 5 matrix (twenty five point filtering) and the weighting factors were obtained from the ^{99m}Tc point source at the appropriate distances from the High Resolution collimator.

A liver phantom was made with simulated lesions of various sizes, shapes and activity ratios and pictures were taken on Polaroid and recorded on magnetic tape.

A comparison of Black and White Polaroid and two modes of colour T.V. display of the raw data and the effect of smoothing and smoothing plus filtering were obtained from the Receiver Operating Characteristic curves using a group of people to look at these pictures. The program for image processing and image display were written in ASSEMBLY language.

The results of the line source studies show that at the surface of Ultra High Resolution collimator the FWHM is 5.8 mm whereas for the High Resolution collimator it is 6.5 mm or in terms of the M.T.F. the spatial frequencies for 10% response are 1.4 and 1.25 cycle/cm respectively.

The study of the effect of the computer matrix on resolution proves that using a 64 x 64 matrix to record the image is inadequate. The resolution is improved by a 128 x 128 matrix and even better up to 1024 x 1024, if available.

The ^{99m}Tc point source study proves that smoothing causes some loss of resolution whereas filtering restores the image closer to the original distribution but creates some artefacts.

From the results of the "liver" phantom studies, the percentage of true positive against false positive at the confidence level "definite" for each method of display are: Polaroid 27/1, T.V. raw data, linear scale 43/2, T.V. raw data statistical scale plus or minus one standard deviation 41/3, T.V. raw data, smoothing 63/3, and T.V. raw data smoothing plus filtering 69/2.

When the raw data is displayed in a statistical scale of plus or minus one standard deviation (full band equals two standard deviations), the detectability is slightly less than that of raw data displayed in linear scale. However, the response of the observers to the colour television display is better than Polaroid at all levels of confidence and if either smoothing or smoothing plus filtering is applied to the unprocessed images, the detectability is improved.

INTRODUCTION

Nuclear medicine is a relatively new and rapidly expanding field dealing with the use of radioisotopes in patients for diagnostic and therapeutic purposes. The major clinical application at this time involves imaging the distribution of intravenously administered isotopes - so called radioisotope imaging which is now applicable to practically all human organs, the lymph system, the skeleton, and the localisation of a variety of neoplasms. A large number of radiopharmaceuticals are used. Some localise in abnormal tissue such as abscesses and tumours to a greater degree than in the surrounding normal tissue. Other radiopharmaceuticals develop relatively lower concentration in abnormal than in normal tissue such as the malignant tissue in the liver (Brown et al, 1974).

In most instances sodium iodide scintillation detectors are used to perform this imaging. The gamma camera is now widely accepted as the optimum instrument for most radionuclide imaging procedures. The major advantage over alternative systems is the relatively high speed of data acquisition and display (Higgins et al, 1968).

The output is generally in the form of photographs, either

Polaroid or transparency, of a sum of single events on the oscilloscope screen of the gamma camera. The other form of display available is the intensity variation on a T.V. raster. An image has a continuous scale of intensities that can be displayed as grey levels, as colour, as a volumetric display, or as contour lines.

The earliest detection theories in the field of radioisotope imaging were concerned with the problem of optimising collimator performance, rather than with the final display of information (Sharp and Mallard, 1974). In the early 1960's, when computers were becoming available in medical institutions, Winkler and Brown (1964) more or less independently described the use of the systems designed to record the radioisotope scan digitally in a form that would allow computer processing. The first successful application of these techniques to patients was published by Brown in 1964.

In static studies, considerable effort has been expended in computer techniques which will process the basic raw data to give alternative displays. The most obvious application is the correction of the image for non uniformity of response of the gamma camera, and routine computer correction of the image is desirable (Glass, 1973). Other investigations of image processing included smoothing and resolution-recovery.

The purpose is to improve the detectability of an abnormality in the scintigraphic image. There is, however, argument about whether such displays really help the physician in interpreting the information obtained during the isotope study (Edwards, 1974).

The second useful purpose of quantification using a computer/camera system is in the analysis of a dynamic function test. The method of obtaining scintigraphic dynamic function information is to record, in an organ of interest, the behaviour of a radiopharmaceutical tracer as a function of time, following a rapid introduction of tracer. A time sequence of images can be obtained which shows the distribution of tracer during the passage of material through the organ. An example is the radioisotope angiocardiogram (Brown et al, 1973). Regions of interest can be defined with the computer such as the four chambers of the heart and great blood vessels. Total counts in each region of interest can be evaluated for each image in sequence and the activity/time curve can be obtained (Jahns et al, 1972).

This work was based on the Varian 620/L-100 minicomputer interfaced to an Ohio-Nuclear R100 gamma camera which uses 37 photomultiplier tubes and yields a high resolution of 5.8 mm FWHM at the surface of the Ultra High Resolution collimator.

The instruments are located at the Department of Nuclear Medicine, Royal Infirmary, Glasgow.

CHAPTER I

EQUIPMENT

1. Ohio-Nuclear R100 Gamma Camera

The crystal is made of sodium iodide (thallium-activated) and coupled to an array of thirty seven photomultiplier tubes arranged in a hexagonal array. The intrinsic resolution of the crystal at 140 keV is 4.7 mm and 2 μsec dead time. The output from the camera detector goes through electronic circuitry that performs several functions. These include pulse height analysis, amplification and X-Y co-ordinate location. The scintillation camera develops three voltages X, Y and Z. The magnitude and signs of X and Y pulses provide positional information to the oscilloscope of the camera.

The Z pulse is a summation of the output of all the photomultiplier tubes and represents the energy of the incident gamma ray. If the magnitude of the Z pulse indicates an energy value acceptable by the pulse height analyser, the X and Y pulses are then passed to the oscilloscope. Two displays are available: one is the persistance oscilloscope for positioning the patient and the other is the standard C.R.T. for Polaroid standard presentation of results.

There are two collimators in use for this work:

(a) Ultra High Resolution 140 keV, Model 14 S18006, Thickness 1.25", 18000 holes, 0.11" septal thickness, and 9.75" hexagonal field size, 0.061" hole size.

(b) High Resolution 140 keV, Model 14 S18010, Thickness 1.0", 18000 holes, 0.061" hole size, 0.011" septal thickness, 9.75" hexagonal field size.

2. Analog-to-Digital Converters (A.D.C.)

The function of the scintillation camera interface is to translate the analog X and Y position signals from the camera, corresponding to the location of a properly detected event, into digital values and to transfer these values to the computer for storage. Two LABEN type 8212 1024 channel A.D.C.'s are used: one for X-position signals and one for Y-position signals, which are activated only upon receiving a signal from the camera indicating that the detected event was within the selected energy range. For a 64 x 64 matrix each generates a 6-bit output. These are combined in a LABEN type 8120 Bidimensional analysis control unit to give a 12-bit word which is transmitted into the computer via the Buffered I/O unit.

3. Varian 620/L-100 Computer

The Varian 620/L-100 is a general purpose digital computer, designed for a variety of system applications. The computer processes 16-bit words and has 16K core memory with a full cycle execution time of 950 nanoseconds. The central processing unit features four user-accessible operation registers, five buffer registers and an overflow indicator. The mainframe optional features included in the computer are multiply/divide and extended addressing, real time clock and power failure restart.

System I/O options include: Priority Interrupt Module (P.I.M.) and 3 Buffer Interlace Controllers (B.I.C.). The Priority Interrupt Module (P.I.M.) allows any peripheral controllers or other device in the system which is connected to it to interrupt Central Processing Unit (C.P.U.) operations to initiate the servicing of interrupt subroutines.

The Buffer Interlace Controller (B.I.C.) permits peripherals to transfer data directly to or from memory at a rate up to 275,000 words per second by implementing a cycle-stealing, Direct Memory Access (D.M.A.) trapping technique.

Basic computer operations are carried out on integers represented in binary form which do not permit the use of fractions. The only arithmetic operations that are possible are integer addition and subtraction. Operation of multiplication and division can be done with the special hardware. Fractional and decimal numbers must be handled in a floating-point format by software. The maximum-sized integer for Varian 620/L-100 is $2^{15}-1$ or 32767 and the most negative number is -32768. The computer operates on single-precision (one word) numbers that contain 15 bits plus a sign bit. The sign bit occupies the most significant bit position (bit 15); zero in this bit denotes a positive number and one, a negative number. Double-precision arithmetic techniques, in which two computer words (32 bits) represent one number allow the processing of larger numbers.

The Varian 620/L-100 computers feature the following addressing modes for increasing program efficiency:

(a) Direct

(b) Indirect

(c) Relative to program counter (P register)

(d) Indexed with the X or B registers

(e) Extended) 2 words addressing

(f) Immediate)

A word is 16 bits long and can contain data, a memory address or an instruction. Programs written in ASSEMBLY language are entered into the computer via the teletype and the Varian 620

D.A.S. assembler translates the mnemonic codes into machine language.

One useful utility program is the Varian 620 AID II debugging program which provides software to facilitate on-line program checkout and correction. It also allows the recording of the binary contents of memory on paper tape or magnetic tape or in a readable format on the teletype and will load object programs from a high-speed or teletype paper tape reader or magnetic tape.

The other useful language which can be used with this minicomputer is BASIC, using a compiler it will translate the program into machine language line by line. It is an easy to use language but, in fact, programs for on-line data processing from the gamma camera cannot be written in BASIC because it is slow and there is insufficient core capacity.

4. Peripheral Devices

(a) Teletypewriter (ASR-33) with paper tape punch and reader.

(b) High-speed paper tape reader with optical (photoelectric) sensor operates at 300 characters per second.

(c) Magnetic tape operates at a fixed speed of 37½ inch/sec while reading and writing information at a speed of 6667 words/sec in binary mode. This is used for gamma camera image storage and program storage.

(d) Colour television (19" SONY TRINITRON) which is for radioisotope image display.

(e) Buffered I/O for input of data from the gamma camera.

5. Digital Colour T.V. Interface

The digital T.V. interface enables a colour T.V. screen to be controlled by a Varian 620 computer. The resulting picture is a square matrix of side length 128 individual units forming, in total 16384 square units. Each unit may be set to one of 16 colours previously selected from a repertoire of 256 colours. A buffer store of 4096 words within the interface holds the data for the entire screen area allowing the desired picture to be displayed without computer intervention. The Buffer store is scanned continuously by T.V. Computer time is only required to alter the picture which can be done during frame flyback. The user can choose to alter part or all of the display, either in the sight of the observer, or by blanking the screen to achieve a higher data rate, or to conceal transient erroneous pictures, for example half the new with half of the old picture. The picture data may be transferred to the interface either by program output or by D.M.A. transfer.

The interface buffer store is a 4096 word 16 bit store. Each word holds four elements called "CHU's" of unit colour data arranged such that the most significant chu is displayed first, the remaining following in natural order. Address zero of the store corresponds to the top left-hand corner of the display. The data is transmitted by the computer in the packed 16 bit format. Its destination address in the store is defined by the store address write counter. This counter may be preset by the computer to any value in the range zero to 4095. The next picture data transmitted will be stored in the present address and having been stored, increment the address. Thus the display may be updated starting from any point on the screen.

Block diagrams of the equipment and picture are shown in Figures 1 and 2. Block diagram of T.V. display from the computer memory is shown in Figure 3.

Figure 1

Block diagram of the equipment.

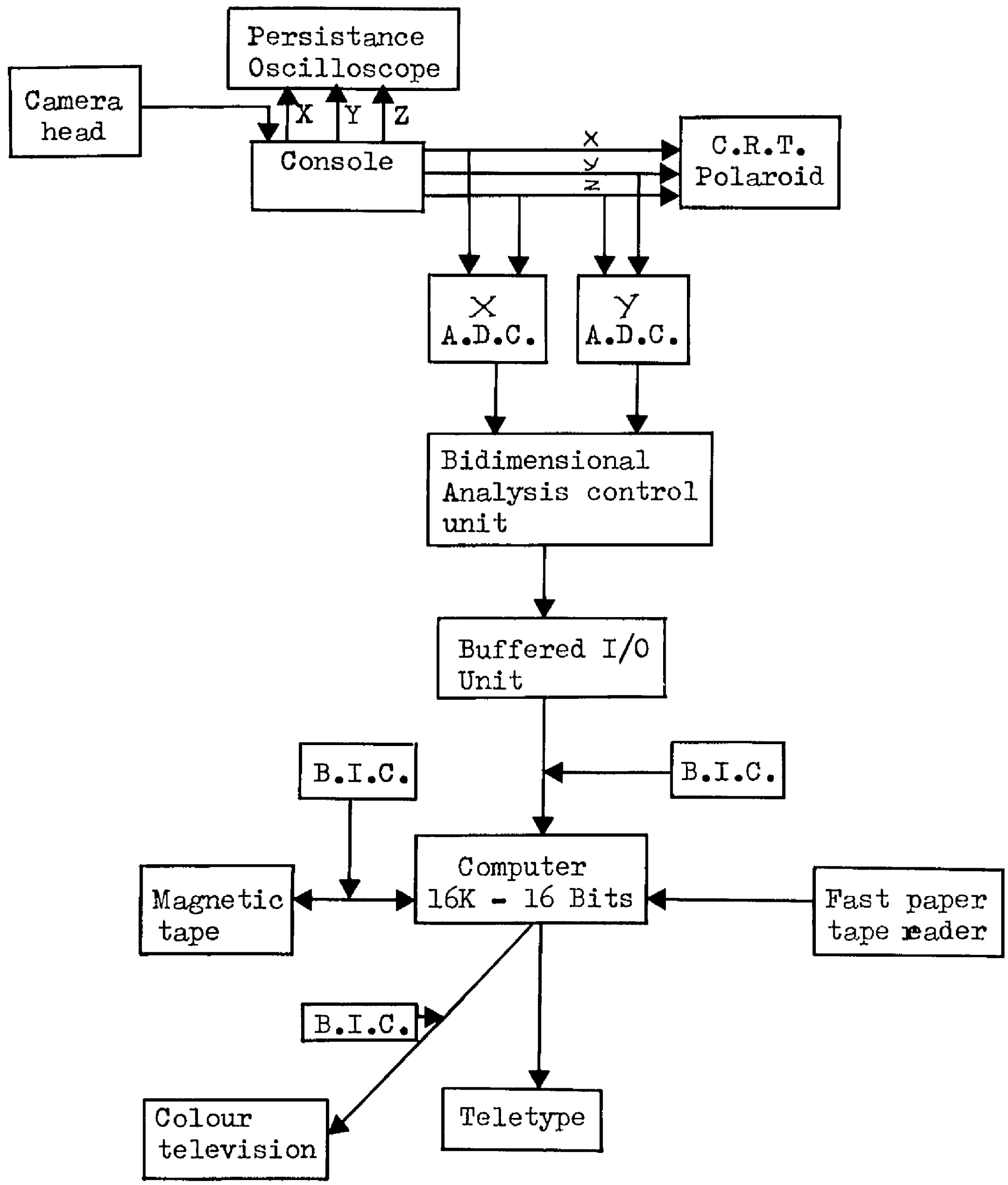
Persistance Oscilloscope
Camera head
X
Y
Z
Console
X
Y
Z
C.R.T. Polaroid
X A.D.C.
Y A.D.C.
Bidimensional Analysis control unit
Buffered I/O Unit
B.I.C.
B.I.C.
Magnetic tape
Computer 16K - 16 Bits
Fast paper tape reader
B.I.C.
Colour television
Teletype

Figure 2

Picture of the equipment.

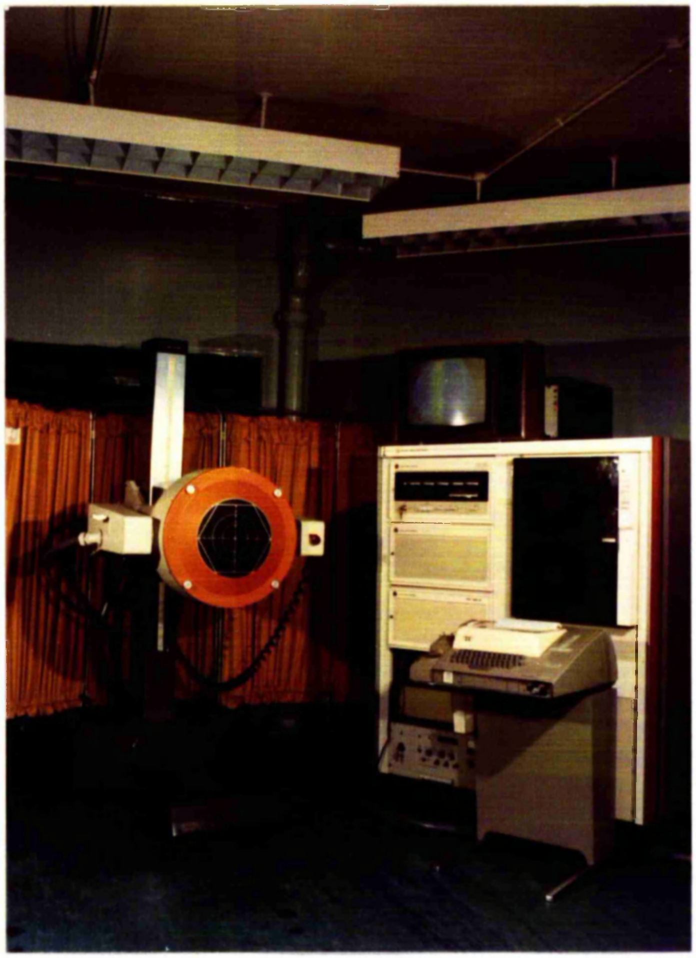

Figure 3

Block diagram of T.V. display from computer memory.

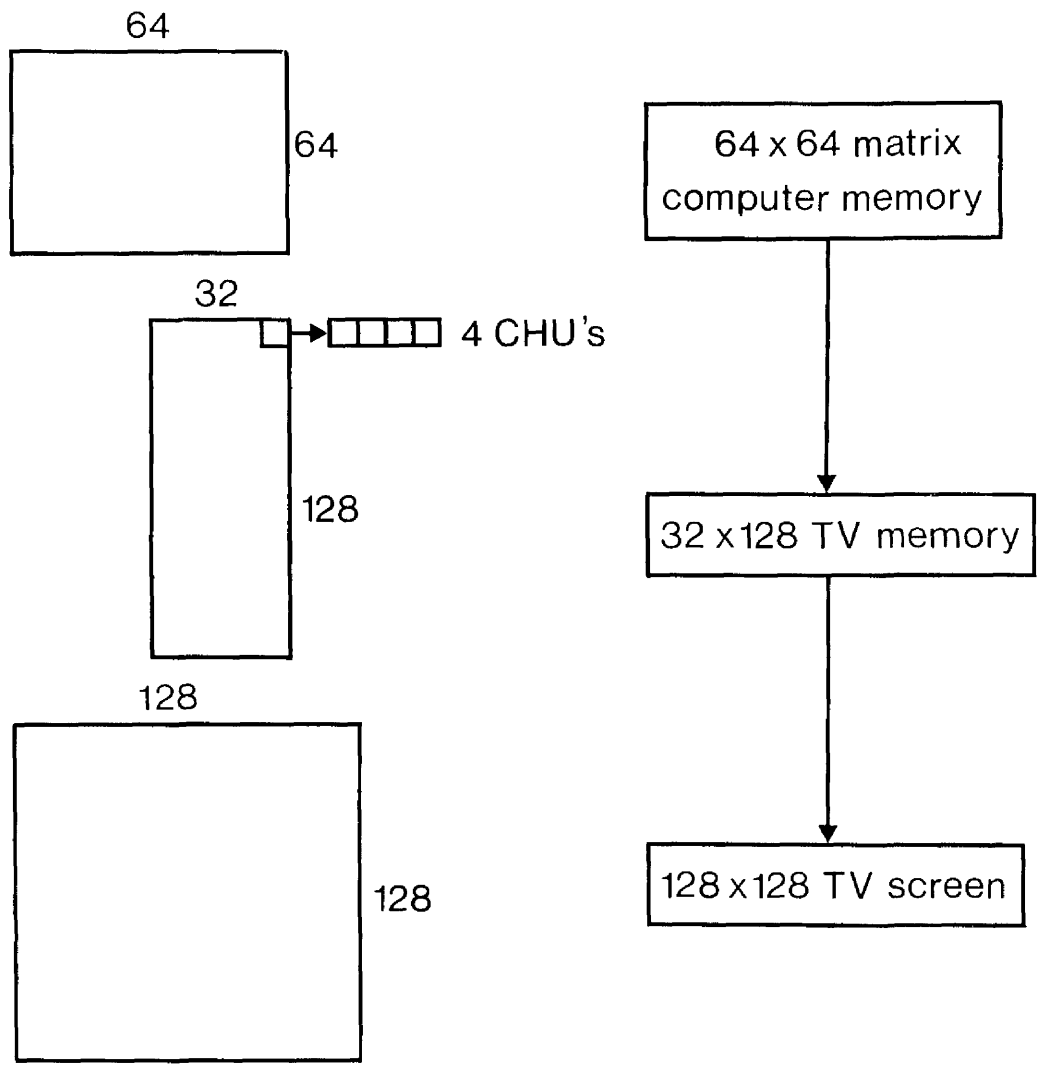
64
64
32
4 CHU's
128
128
128
64 x 64 matrix computer memory
32 x 128 TV memory
128 x 128 TV screen

CHAPTER II

ROUTINE DATA COLLECTION, PROCESSING AND IMAGE DISPLAY

1. Data Collection

For scintigraphic images the core memory of the computer is regarded as a matrix of 64 x 64 or 4096 locations, meaning that the area looked at by the camera is broken into 4096 discrete areas, each about 4 mm square. An individual location in core memory is assigned to a particular X, Y address in the image matrix. When a scintillation is detected in one of these areas, the contents of that part of the matrix in the computer is incremented by one.

Using the routine gamma camera program data may be gathered into memory for either a given period of time, or a given number of counts, either way being easily specified by the operator, via the conversational program at the time of examination. Once the data is in the computer in matrix form it may be either rapidly transferred to magnetic tape store (the rate of transfer is 6667 words of information per second), or if required may be analysed immediately. This analysis is done without further references to the gamma camera. The raw data is displayed on the screen of the gamma camera oscilloscope and the raw or manipulated data is displayed on colour television. Control of all functions is via the teletype, using coded commands, but on occasions extra control may be exerted through switch registers on the front panel of the computer.

For dynamic studies, the images were recorded in the preset time mode. The shortest time available is 1 frame per 0.5 second. If necessary, a few successive images can be added together to form an image with more counts for defining of regions of interest, or two successive images can be subtracted from each other to emphasize changes in the image.

2. Uniformity Correction

The purpose of uniformity correction is to compensate for the difference in sensitivity over different parts of the crystal face. The correction coefficients are obtained from a uniform plane source. The corrected image consists of a matrix, each element of which is the product of an element from the data matrix and corresponding element from the correction coefficient matrix. Camera non uniformity changes with time and also window setting, so new uniformity field image was obtained every day, at approximately the same average count rate as is encountered in the patient studies (Figure 4).

The use of the 16K of computer memory is as shown in Figure 5. The first 4K of the memory contains the routine gamma camera program. This program is used routinely for data acquisition and data processing both "on line" and "off line". The second 4K of the memory is designed to be the picture area in the matrix form of 64 x 64. The address range is 010000-017777 (octal). The third 4K of the memory is designed to be the uniformity correction field. The fourth 4K of the memory is designed for the image processing program which starts at 030000 and not further than 035777 because the utility program AID II is usually a permanent program which resides on this 4K and starts at address 036000.

The image processing program can be called from the routine gamma camera program by a special command "J" and return to the routine gamma camera program is by the command "GC" (Figure 6).

3. Image Display

The display program is used to present images for interpretation. The computer generates different colours according to the counts in each element of the matrix of the picture. The display need not contain the same number of elements as the matrix stored in the computer. A finer display can be prepared from the image matrix by interpolating between the matrix points. This gives a subjectively much more acceptable picture.

Two programs of image display were written in ASSEMBLY. These are 64 x 64 image display and 128 x 128 image display from the 64 x 64 computer memory.

a) <u>64 x 64 Image Display</u>

The counts in one picture elements of the computer memory are used to determine the colour of a block of four adjacent picture elements on the T.V. display (128 x 128), thereby producing an effective matrix of only 64 x 64 elements on the T.V. display (Figure 7a). The program for this type of display is included as Appendix 2.

b) <u>128 x 128 Image Display from the 64 x 64 Computer Memory</u>

The counts from 4096 elements of 64 x 64 array in the computer memory are displayed as alternate points in alternate line of 128 x 128 television display. The remaining points on each line of the T.V. display are calculated as the average of the intervening lines of adjacent points. Similarly, the intervening lines of the T.V. display are calculated as the average of the line above and the line below (Figure 7b). The program for this type of display is part of the image processing program (Appendix 1).

4. Display Colour Coding

The colour display on the television is arranged both on a conventional linear scale and statistical scale.

a) Linear scale

The counts in the picture are divided into 15 equal bands and the colour is defined by a number which ranges from 0-15 as seen in the colour spectrum (Figure 8).

$$\text{One colour width} = \frac{\text{Maximum counts} - \text{Minimum counts}}{15}$$

Normal display assumes that the minimum counts equal zero. However, both minimum counts and maximum counts may be changed by Teletype commands for background subtraction and contrast enhancement or contouring.

b) <u>Statistical Scale</u>

The statistical nature of the image information may be allowed for by choosing the width of the colour bands to be proportional to the standard deviations of the mean counts in each band.

There are two choices of statistical scale in the image display program. The total width of each colour band can be calculated for one standard deviation or two standard deviations.

The flow chart of the colour scale display controlled by external sense switch is shown in Figure 9.

5. <u>Calculation of the band width of N standard deviations</u>

MAX 1 ____________

C ____________

MAX 2 ____________

MAX 1 = the maximum count of a picture.

C = centre value of top band.

MAX 2 = lower level of the top band.

N = number of standard deviations in half the band width.

Therefore:

$$\text{MAX } 1 = C + N\sqrt{C}$$

or

$$C^2 - (2\text{ MAX } 1 + N^2)\, C + \text{MAX } 1^2 = 0 \qquad -(1)$$

That is:

$$C = \text{MAX } 1 + \frac{N^2}{2} \pm \frac{N}{2}\sqrt{4\text{ MAX } 1 + N^2}$$

$$\text{MAX } 2 = \text{MAX } 1 + N^2 \left(1 - \sqrt{\frac{4\text{ MAX } 1}{N^2} + 1}\right) \qquad -(2)$$

If the full band width equals two standard deviations, that is $N = 1$

$$\text{MAX } 2 = \text{MAX } 1 + 1 - \sqrt{4\text{ MAX } 1 + 1} \qquad -(3)$$

The lower level of the next band is calculated by substituting MAX 1 by MAX 2 in equation (3) and so on until either fifteen bands have been defined or a lower level of zero has been found. These fifteen band maxima are kept in fifteen locations and each picture element is coded by comparison with this series of values.

CHAPTER III

PERFORMANCE ANALYSIS OF IMAGING SYSTEM

There are two major sources of degradation in radionuclide imaging. There is the finite resolution of the imaging device and the statistical fluctuations, sometimes called "noise", that arises because of the random process of the radioactivity and limited quanta making up a scan (Gustafssan, 1972).

1. Measurement of Resolution

The spatial response of an imaging system is measured by placing a single point source at an appropriate distance in front of the detector. A scan of this point is made and a response curve of this point is called the point spread function which will approximate a gaussian or normal distribution. The width of the curve at half maximum (FWHM) will be used as a measure of the resolution of the detecting system.

While the point spread function is a quantitative measure of the response of the system, a line source is often more convenient to use. If the point response curve is gaussian it can be shown that the pattern as one scan across a line source is also a bell-shaped gaussian distribution, with the same full width at half maximum. If a cross section of the image of the line source is plotted, such a curve is called a line spread function (Aronow, 1973). The line spread function leads to a mathematically useful concept called Modulation Transfer Function (M.T.F.).

An intensity distribution of radioactivity can be thought of as being made up of a linear combination of sinusoidal components at various spatial frequencies. An image represented as the intensity at each spatial position is said to be represented in the "space domain". When the image is represented by the amplitude of each sinusoidal component, it is said to be represented in the "frequency domain". These two representations are completely equivalent, and it is possible to go from one to the other by Fourier Transform and the inverse Fourier Transform (Pizer et al, 1974). In the frequency domain, the performance of the scintigraphic instrument is expressed in terms of the Modulation Transfer Function (M.T.F.). Points on the M.T.F. may be regarded as the ratio of the amplitude of a sinusoidal wave in the image to the amplitude of the sinusoidal wave of corresponding spatial frequency in the source.

At each frequency (ν) the M.T.F. can be mathematically calculated from the line spread function. The M.T.F. is simply the normalised Fourier Transform of line spread function, (Boyd et al, 1974). The calculation of M.T.F. for all frequencies can be done by the computer. This transform is given as

$$\mathrm{MTF}(\nu) = \frac{\int_{-\infty}^{\infty} L(x)\cos(2\pi\nu x)\,dx}{\int_{-\infty}^{\infty} L(x)\,dx}$$

$L(x)$ = Line spread function

x = Displacement from the centre of the line spread function

ν = Spatial Frequency

If the system is high-fidelity, the M.T.F. would equal 1 out to the high spatial frequencies, but ordinarily the system acts as a low pass filter. That is, it responds to broad patterns (low spatial frequencies) but not to fine detail (high spatial frequencies).

The program for this calculation is included as Appendix 3.

2. Effect of Computer Matrix on Resolution

Each element of the 64 x 64 matrix in the core memory of the computer represents about 4 mm square in the object while the resolution of the camera and the Ultra High Resolution is about 5.8 mm FWHM at surface. This means there is some loss of resolution by the computer matrix. To determine the effect of the computer matrix on resolution the gain of the system was adjusted at the A.D.C.'s. Normally when the A.D.C.'s gain are adjusted to 1, the gain of the rest of the system is such that the field of view of the gamma camera occupies a 64 x 64 matrix in computer core. When the A.D.C.'s gain are adjusted to 2, 4, 8 or 16 it means that the full gamma camera field occupies a memory matrix of 128 x 128, 256 x 256, 512 x 512 or 1024 x 1024 elements if available.

In case of 16 times normal gain (gain 1), the resolution of the total system is close to the resolution of the gamma camera plus collimator because the matrix is fine and the discrete nature of the computer storage has little effect on the resolution.

Materials and Methods

A plastic tube (diameter less than 2 mm, 10 cm long) was filled with ^{99m}Tc and then stretched to form a good line source and placed on the surface of the collimator along the

Y direction of the gamma camera. The gain of the A.D.C. in X direction was adjusted to 16 times normal to eliminate the effect of computer matrix and the back bias was adjusted so that the broadened image of the line source, lying in Y direction, was in the centre of the display.

Using the routine gamma camera program the data for a preset count of 300,000 was obtained, uniformed and stored on the magnetic tape. The line spread function was obtained by profiling the image and the curves of line spread function and M.T.F. were plotted. The same method was applied for distances of 5 cm and 10 cm from the collimator.

The data were obtained in the same way for the High Resolution collimator and Ultra High Resolution collimator. To examine the effect of coarser matrices on the M.T.F. the gain of the X A.D.C. only was set to 1, 2 and 4 times normal gain using the High Resolution collimator and the procedure was repeated. The M.T.F.'s were derived from these images in the same way as for the A.D.C. gain of 16.

Results and Discussion

From the experiments on the ^{99m}Tc line source with the X A.D.C. gain adjusted to 16 times normal, the results are plotted in Figures 10, 11 and 12a, and the comparison of the FWHM for the two collimators is in Table 1. For the coarser matrices, with the X A.D.C. gain adjusted to 1, 2 and 4, the results are plotted in Figure 12b.

The FWHM of the line spread function can be used as an index of resolution. It has the advantage that it provides a single number to describe the spatial resolution of a collimator system. However, the performance of an imaging system is more generally described in terms of M.T.F. because it gives more detail about the response at each frequency. Objects and images with fine details and sharp boundaries generally include relatively high frequencies, whereas those with coarse detail mainly include low spatial frequencies (Hine and Erickson, 1974).

The FWHM at the surface of the Ultra High Resolution and the High Resolution collimator are 5.8 mm and 6.5 mm. The 10% spatial frequencies response at surface are 1.40 and 1.25 cycle/cm respectively. This 10% frequency is the highest spatial frequency which is usefully reproduced.

The 10% spatial frequencies response of the High Resolution collimator with gain 1, 2, 4 and 16 are 0.7, 1.0, 1.15 and 1.25 cycle/cm respectively. This can be used as an index to determine the resolution of the system. It is clear that there is much better resolution on a 128 x 128 matrix than on a 64 x 64 matrix and even slightly better resolution with the finer matrices up to 1024 x 1024, if available. Therefore, a 128 x 128 matrix is suggested to record the image to improve the resolution for this system. Lack of memory capacity prevents the use of finer matrices. For small objects or organs such as thyroid, the gain of the system can be adjusted to 2 or 4 in both directions but this cannot be applied to the bigger organs such as liver, brain or lungs, because the field of view of the gamma camera cannot cover the entire organ.

Table 1. Line Spread Functions of ^{99m}Tc (gain 16).

Comparison of FWHM for two collimators

Distance from the surface	High Resolution Collimator (mm)	Ultra High Resolution Collimator (mm)
Surface	6.5	5.8
5 cm	8.5	7.0
10 cm	11.0	8.5

Figure 4

Pictures of uniformity disc before and after correction.

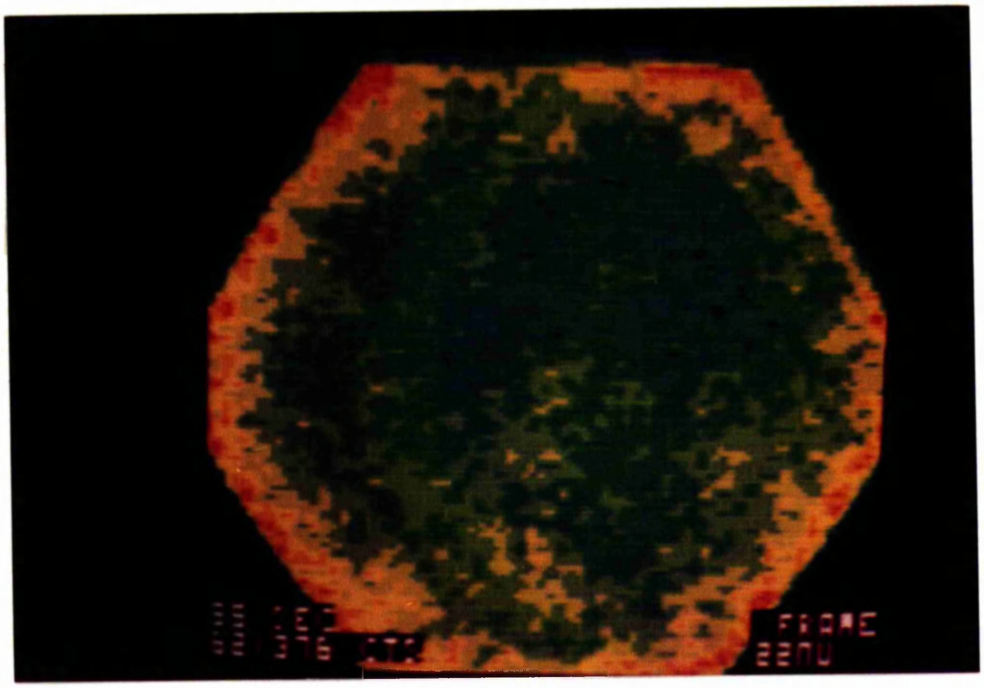

before

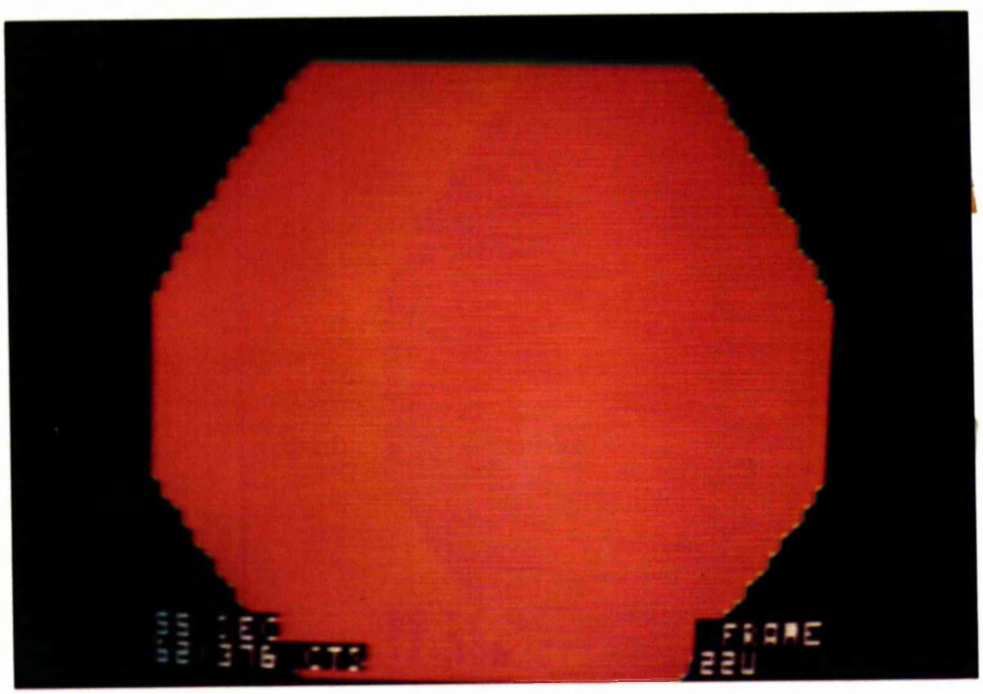

after

Figure 5

Block diagram of the use of 16K computer memory.

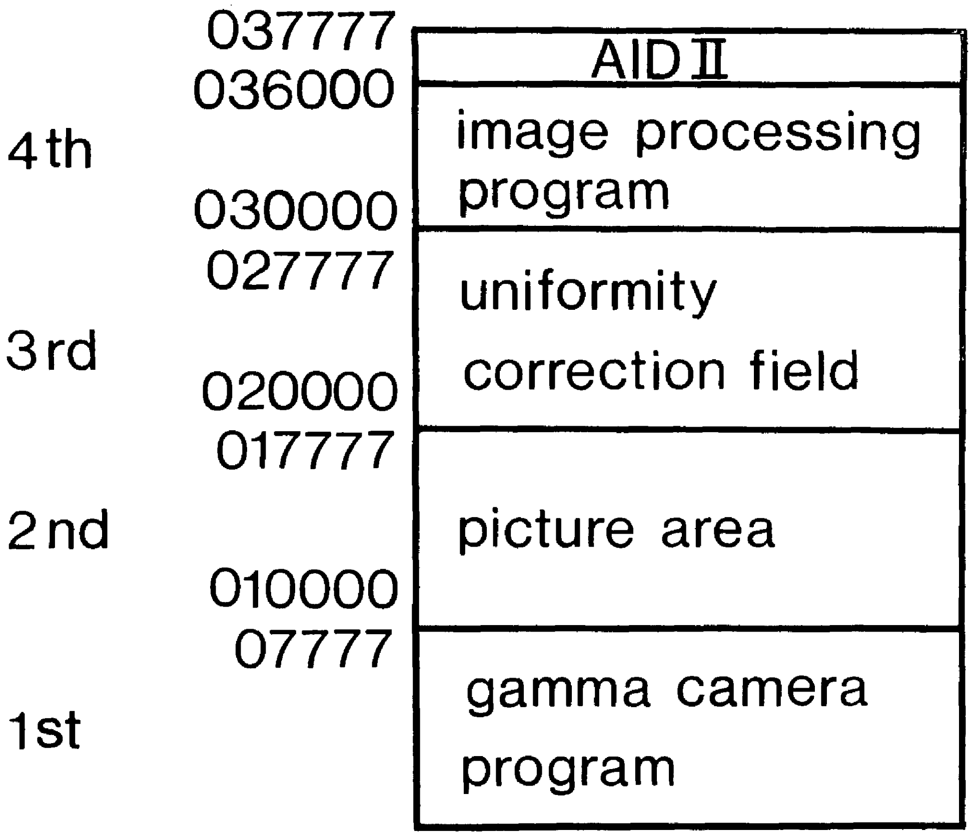
037777
AID Ⅱ
036000
4th
image processing program
030000
027777
3rd
uniformity correction field
020000
017777
2nd
picture area
010000
07777
1st
gamma camera program

Figure 6

Flow chart of the image processing program.

Image Processing Flowcharts

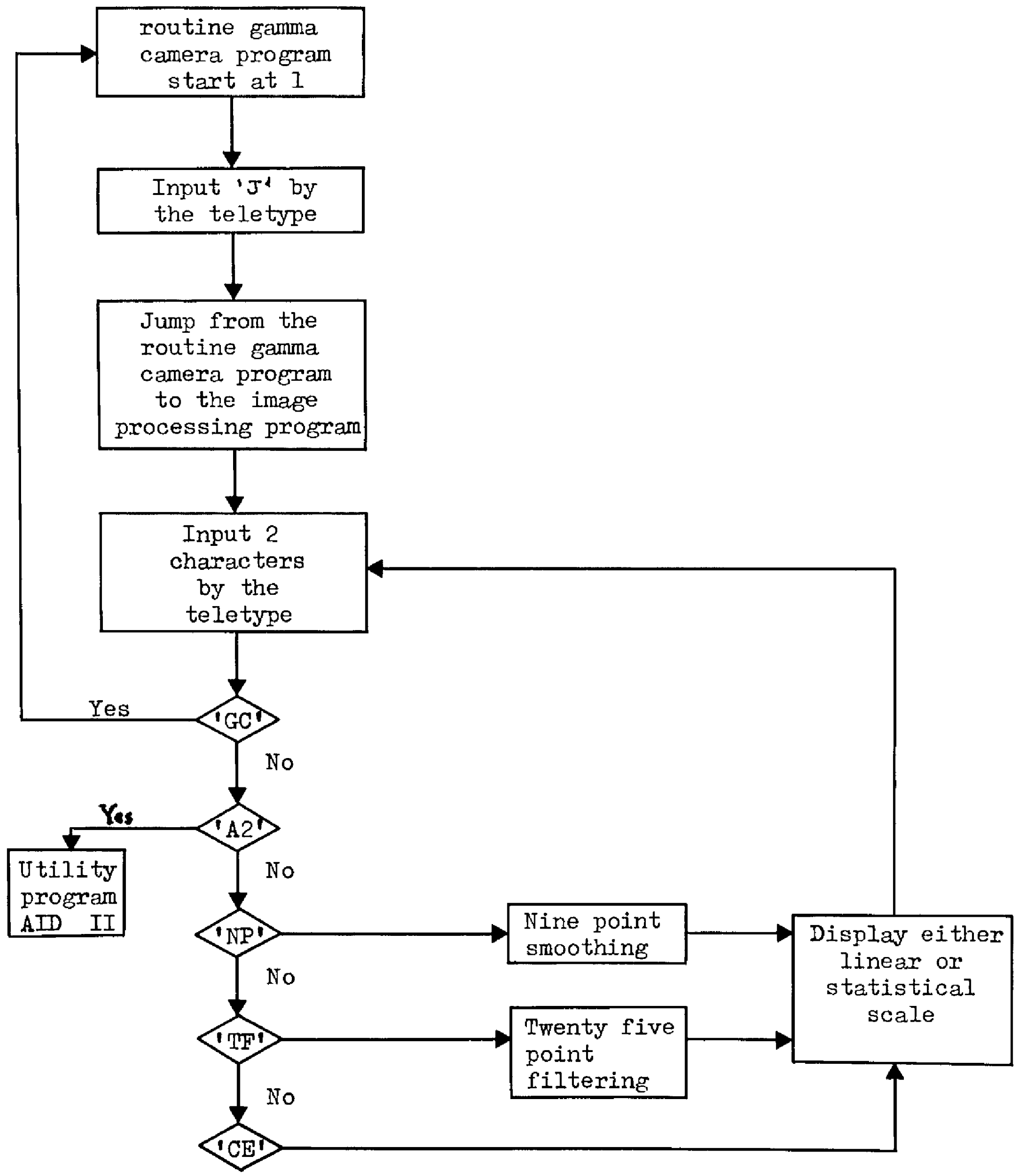

Figure 7

(a) Block diagram of 64 x 64 image display.

(b) Block diagram of 128 x 128 image display from 64 x 64 computer memory.

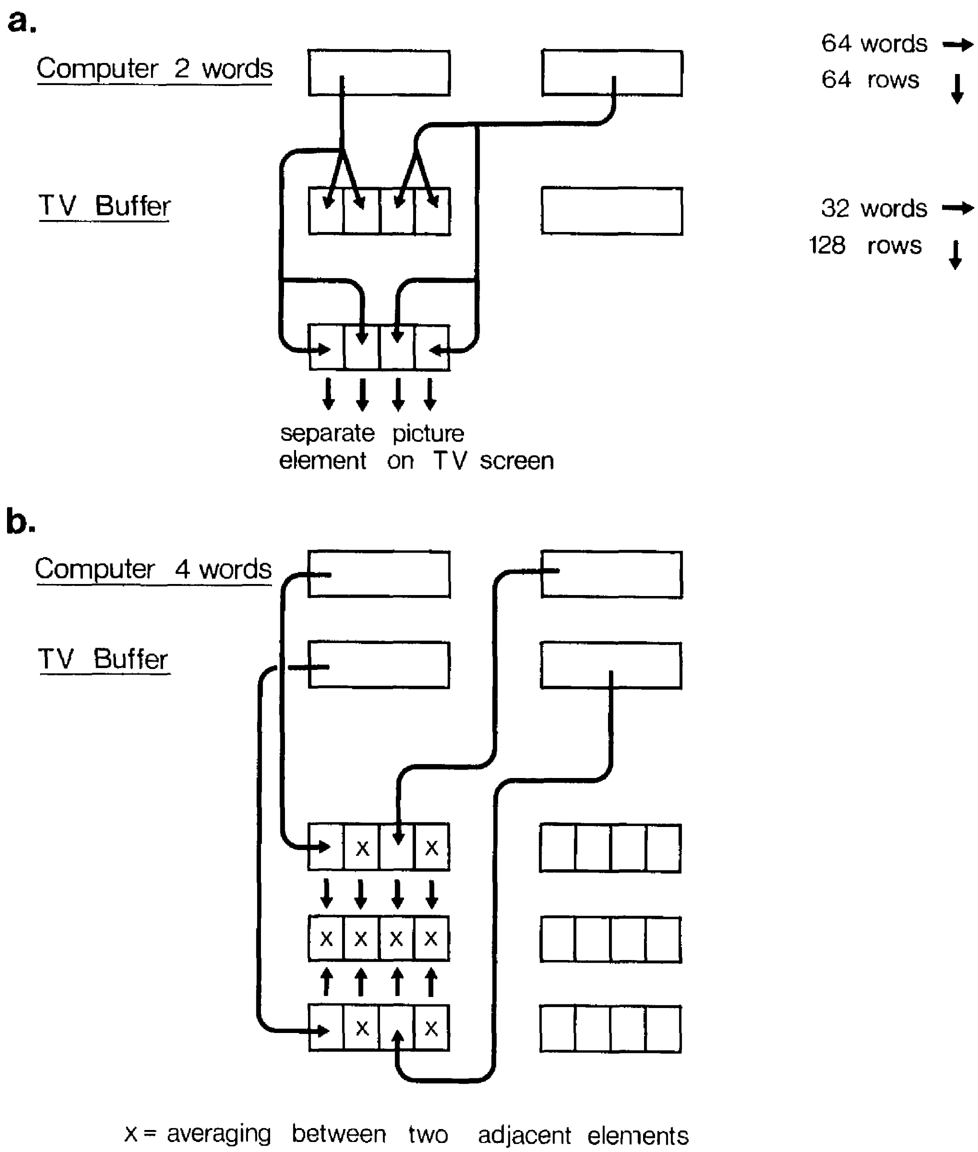
a.
Computer 2 words
64 words
64 rows
TV Buffer
32 words
128 rows
separate picture
element on TV screen
b.
Computer 4 words
TV Buffer
x
x = averaging between two adjacent elements

Figure 8

Picture of colour spectrum.

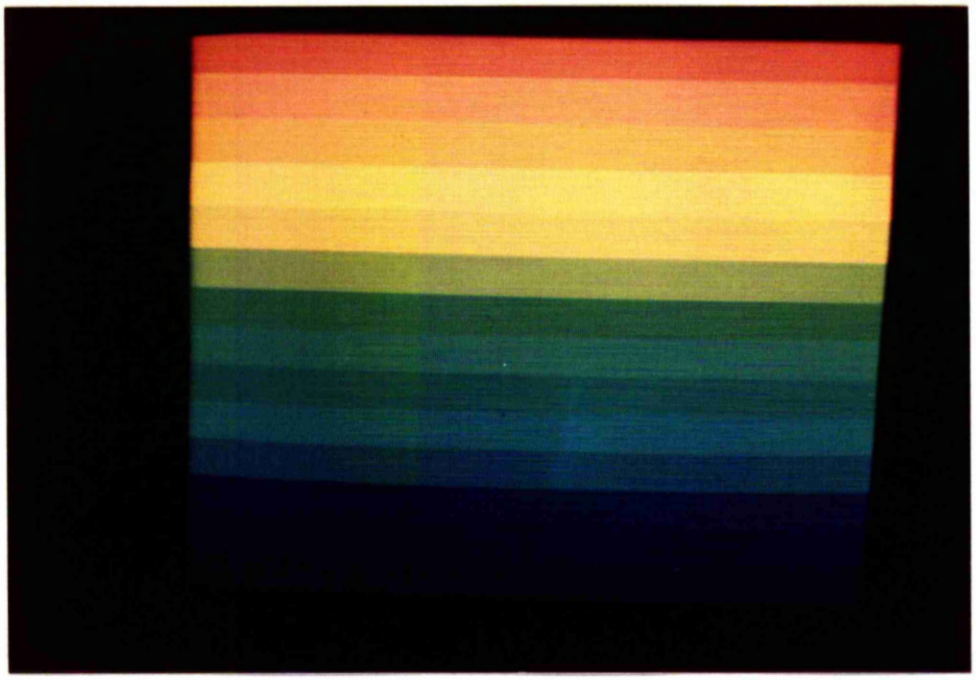

15

0

Figure 9

Flow chart of the colour scale display.

Display flowchart

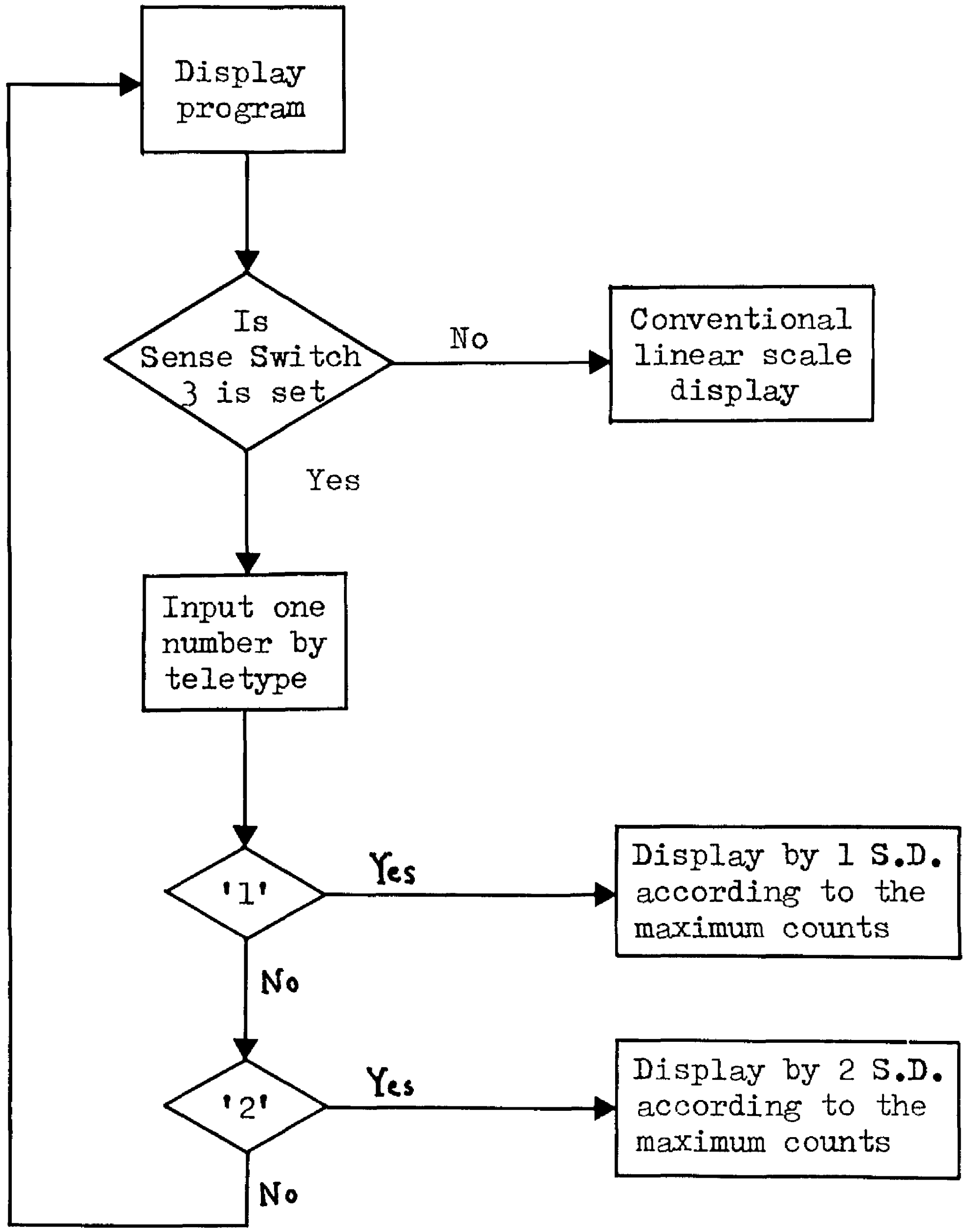

Figure 10

^{99m}Tc line spread functions and M.T.F.'s at various distances from the High Resolution collimator (gain 16).

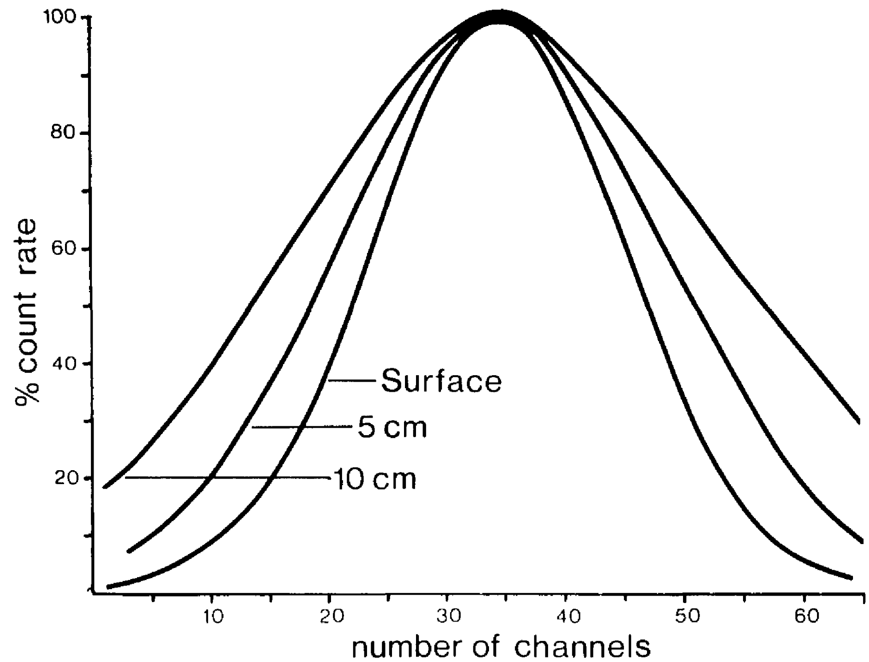
100
80
60
40
20
% count rate
Surface
5 cm
10 cm
10
20
30
40
50
60
number of channels

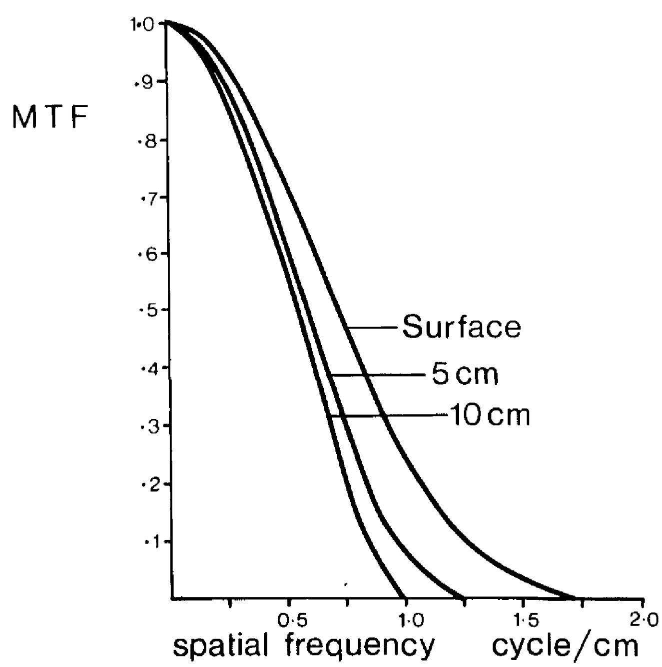
MTF
1·0
·9
·8
·7
·6
·5
·4
·3
·2
·1
Surface
5 cm
10 cm
0·5
1·0
1·5
2·0
spatial frequency
cycle/cm

Figure 11

^{99m}Tc line spread functions and M.T.F.'s at various distances from the Ultra High Resolution collimator (gain 16).

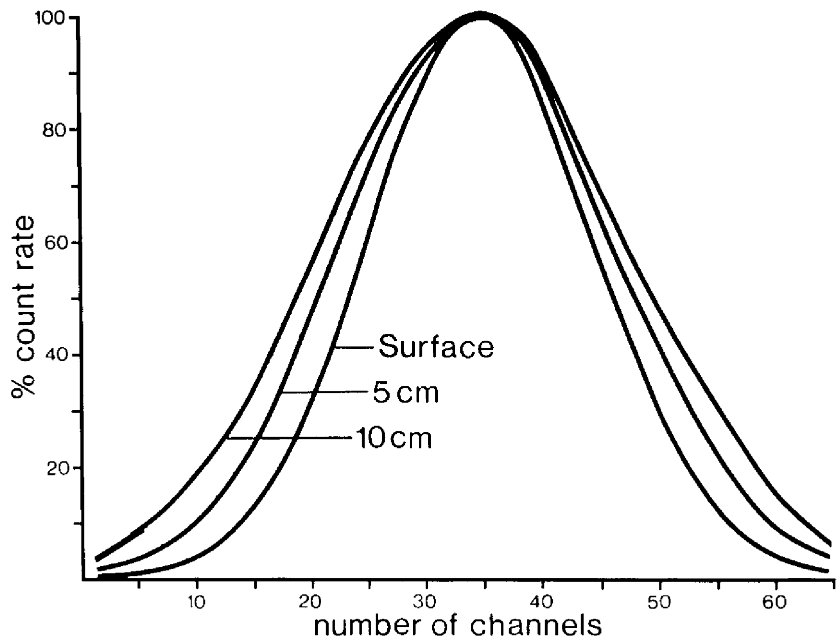
100
80
60
40
20
% count rate
10
20
30
40
50
60
number of channels
Surface
5 cm
10 cm

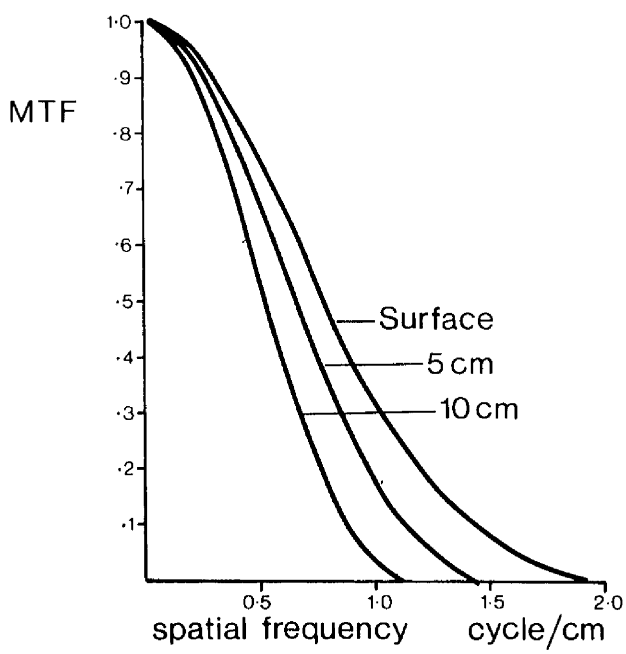
MTF
1·0
·9
·8
·7
·6
·5
·4
·3
·2
·1
0·5
1·0
1·5
2·0
spatial frequency
cycle/cm
Surface
5 cm
10 cm

Figure 12

(a) Comparison of M.T.F.'s at the surface of two collimators.

(b) Comparison of M.T.F.'s at various gains at the surface of the High Resolution collimator.

(a)

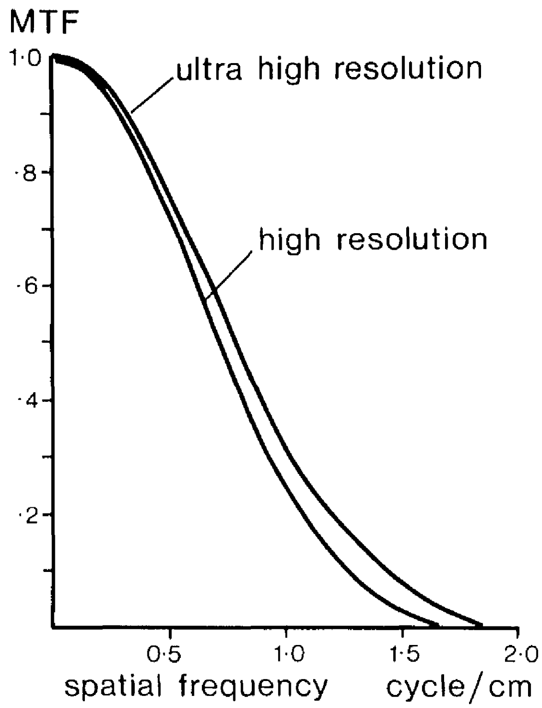
MTF
1·0
·8
·6
·4
·2
ultra high resolution
high resolution
0·5
1·0
1·5
2·0
spatial frequency
cycle/cm

(b)

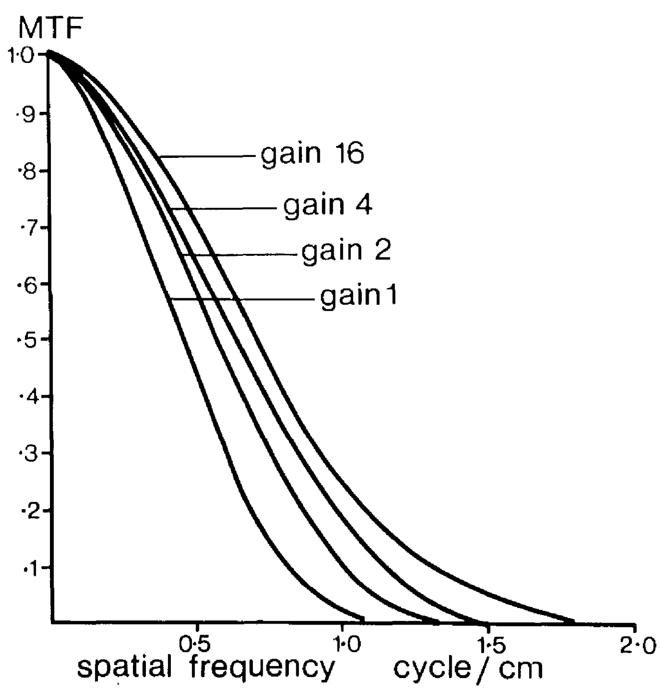
MTF
1·0
·9
·8
·7
·6
·5
·4
·3
·2
·1
gain 16
gain 4
gain 2
gain 1
0·5
1·0
1·5
2·0
spatial frequency
cycle/cm

CHAPTER IV

IMAGE ENHANCEMENT

In theory the ability to detect small lesions in a radionuclide image can be improved by computer processing. The process of removal of high frequencies noise is called "Smoothing". Having enhanced the image by removing the statistical fluctuations, the image will be degraded as a result of limited resolution of the detector as demonstrated by the M.T.F. (Chapter III). The process to refocus the image because of the limited resolution is called "Resolution-recovery" (Pizer et al, 1974).

Smoothing and Resolution-recovery are, generally speaking, inversely related. Therefore, image enhancement methods are the combined effects of these two processes, the relative properties of each depending on the statistical quality of the particular image data.

1. Smoothing

The process of smoothing is to replace each element of the original matrix by a positively weighted average of the intensity of itself and neighbouring elements. A simple method is nine point smoothing (Mould and Wyld, 1973). Many investigators have suggested various functions for smoothing, for example:

a) $$\begin{bmatrix} 1 & 1 & 1 \\ 1 & 1 & 1 \\ 1 & 1 & 1 \end{bmatrix} \div 9$$

which has been used by Nakamura et al (1973).

b) $$\begin{bmatrix} 1 & 2 & 1 \\ 2 & 4 & 2 \\ 1 & 2 & 1 \end{bmatrix} \div 16$$

which is the digital analogue of a "low pass electrical filter" and has been used by Keyes et al (1973) and Bell and DeNardo (1970).

The flowchart of nine point smoothing is shown in Figure 13.

2. Resolution-recovery

Resolution-recovery can be done on any size of matrix but this work is restricted to a 5 x 5 matrix. In contrast to smoothing, a set of positive and negative weighting factors is used. The weighting factors for this filter can be obtained from the appropriate point spread function as described below. Initially, weighting factors were calculated which restored the image to be the ideal point, that is, after processing the point image, the neighbouring elements are zero and the centre elements contains all the counts. However, using these weighting factors with the phantom or clinical data enhances the high frequency noise too much and increases the mottling, even after considerable previous smoothing. A second less demanding approach was, therefore, tried. The enhancement matrix was designed to convert the image of a point-distribution at a distance from the collimator into the point spread function at the surface of the collimator.

3. Calculation of the Weighting Factors

Assume that the distribution of the image of a point source distant from the collimator is within a 5 x 5 matrix and the maximum count is at the centre point. The correction matrix (Figure 14) consists of a set of constants K1, K2, K3, K4, K5 and K6 acting upon this uncorrected image matrix so that the resulting distribution of all elements is in proportion to the distribution of the image of a point source at the surface of the collimator. This will lead to six equations with six unknowns, which are solved by matrix inversion (Cahill and Lawrence, 1970). This set of weighting factors can be worked out easily by a minicomputer with a simple language, BASIC. The program for this calculation is as in Appendix 4.

Materials and Methods

A point source of ^{99m}Tc (diameter less than 2 mm) was dropped on a thin aluminium foil tray which was placed on the surface of the High Resolution collimator. The counts of the point source were acquired and stored on the magnetic tape by the routine gamma camera program. The result was uniformed and the data were printed out to obtain a point spread function. The same method was applied at the distance of 5 cm and 10 cm from the surface of the collimator.

Using water as a medium between the point source and the collimator, at the distance of 5 cm and 10 cm, the data were obtained in the same way as in air.

The point source response at 10 cm from the High Resolution collimator (in air) was used to determine the effect of smoothing and filtering. Using the gamma camera profiling program applied to this point source image the data shown in Figure 16 was obtained. The same process was used when a smoothing function and appropriate filter were applied. The smoothing function is:

$$\begin{bmatrix} 1 & 1 & 1 \\ 1 & 1 & 1 \\ 1 & 1 & 1 \end{bmatrix}$$

The filter is of the form of Figure 14 with

$$\begin{aligned} K1 &= 2.498 \\ K2 &= 0.182 \\ K3 &= -1.139 \\ K4 &= -0.208 \\ K5 &= 0.333 \\ K6 &= -0.006 \end{aligned}$$

An additional experiment was carried out using the Williams liver phantom (Figure 17) filled with ^{99m}Tc, placed at 10 cm from the High Resolution collimator. A preset count of two million was acquired and stored on the magnetic tape. A smoothing function of low pass filter 4, 2, 1 was applied to the image of this phantom, twice, to reduce fluctuations, followed by the filter obtained from 10 cm ^{99m}Tc point source, once, to enhance the high frequencies. The profiles across the hot spots and cold spots were obtained.

The data on this liver phantom on the surface of the same collimator was obtained in the same way as at 10 cm. Without filtering, the same smoothing function was applied to the image of the phantom and profiles across both cold and hot spots were obtained for comparison with those of the phantom at 10 cm with filtering.

Results and Discussion

The process of smoothing reduces the random variation of the radioisotope images but at the same time it causes some loss of resolution. However, a filter function corrects for the effect of the imaging system and restores the image closer to the original distribution, obtaining greater resolution (MacIntyre, 1972).

The number of points to be considered in smoothing depends on the statistical nature of the data. If the statistics of the image are very poor it may be necessary to use twenty five point smoothing to produce acceptable quality. However, in all normal static clinical studies, nine point smoothing proves to be adequate. The smoothing procedure can be repeated as often as required in order to provide the degree of smoothing considered necessary (Vernon and Glass, 1971).

In the absence of noise the filtering operation could be carried out exactly as described in theory. However, an observed scan represents not only the actual nuclide distribution but also a considerable amount of additive "noise" due to the random nature of radionuclide decay. This noise greatly complicates the practical considerations involved in correcting the scan by filtering. If one attempts to do filtering on raw data, the result is degraded due to amplification of this noise. Thus, some prior smoothing is necessary.

This was required in the phantom study where two million counts were accumulated. A clinical study usually has only a fraction of this number of counts, making smoothing even more necessary before filtering is attempted.

From the experiments on the ^{99m}Tc point source, the point spread functions were obtained and results are tabulated in Table 2 and Figure 15. This leads to the calculation of a set of weighting factors for image enhancement. Four examples of these weighting factors are tabulated in Table 3.

To determine the effects of smoothing and filtering on ^{99m}Tc point source, the profile curves were plotted in Figure 16.

The FWHM of the raw data, after smoothing and after filtering are 10.4, 14.4 and 6.4 mm respectively. It is clearly seen that smoothing causes some loss of resolution whereas filtering narrows the point spread function at half maximum but also creates side wings to the response which can cause artefacts.

The results from the Williams liver phantom are plotted in Figure 18 and Figure 19. From Figure 18, the profiles across both cold and hot spots after smoothing and smoothing plus filtering at the same distance (10 cm), show that at low frequencies as shown by larger defects, the resolution is degraded and at higher frequencies as shown by smaller defects the resolution is improved. Figure 19, which is the comparison between the profiles across cold and hot spots at the surface and at 10 cm, is a complementary result to Figure 18.

Two colour Polaroid pictures, as shown in Figure 20, show the smallest defect appears larger after filtering corresponding to the profile curves in Figure 18. Thus, filtering improves the detectability of small defects.

Table 2. Point Spread Functions of ^{99m}Tc on the High Resolution Collimator (gain 1)

Distance from the central point (mm)	% counts at surface (air)	% counts at 5 cm (air)	% counts at 10 cm (air)	% counts at 5 cm (water)	% counts at 10 cm (water)
0	100	100	100	100	100
4	40	59	69	56	70
5.66	16	34	50	32	48
8	3	11	26	12	24
8.94	1	6	19	7	17
11.31	0	1	7	2	6

Table 3. Weighting Factors for Spatial Frequency Filtering Obtained from the Point Spread Functions at Various Distances from the High Resolution Collimator (gain 1)

Constants	5 cm (air)	10 cm (air)	5 cm (water)	10 cm (water)
K1	1.244	2.498	0.922	3.187
K2	2.800	0.182	0.367	-0.039
K3	-3.249	-1.139	-0.603	-1.359
K4	-2.474	-0.208	-0.265	-0.820
K5	2.440	0.333	0.286	1.09
K6	-1.624	-6.234 E-03	-0.132	-0.670

Figure 13

Flow chart of nine point-smoothing.

Nine-point smoothing flowchart

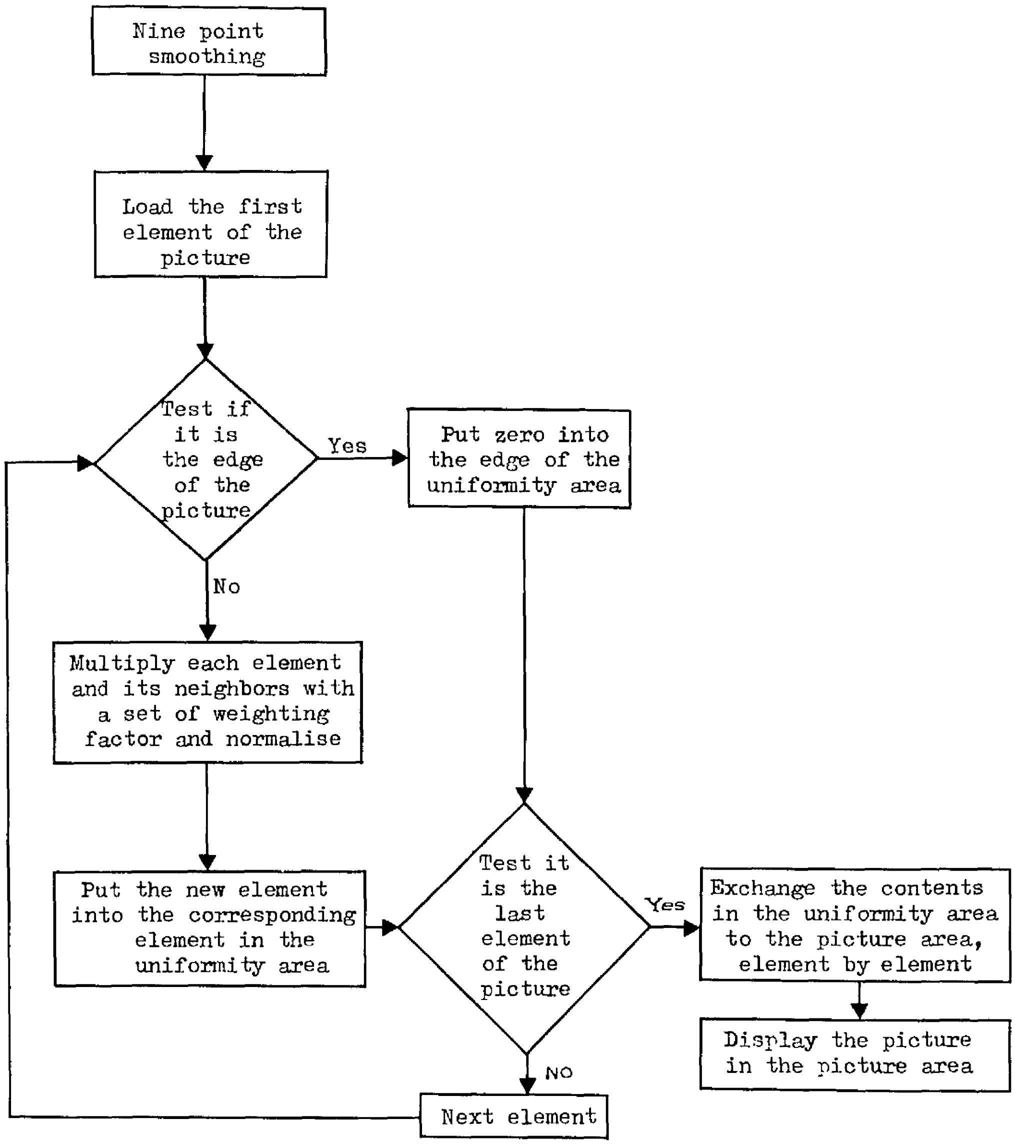

Figure 14

Block diagram of a set of weighting factors acting upon the uncorrected image matrix.

K6	K5	K4	K5	K6
K5	K3	K2	K3	K5
K4	K2	K1	K2	K4
K5	K3	K2	K3	K5
K6	K5	K4	K5	K6

Figure 15

(a) Point spread functions of ^{99m}Tc at various distances from the surface of the High Resolution collimator (air).

(b) Point spread functions of ^{99m}Tc at two distances from the surface of the High Resolution collimator (water).

(b)

(a)

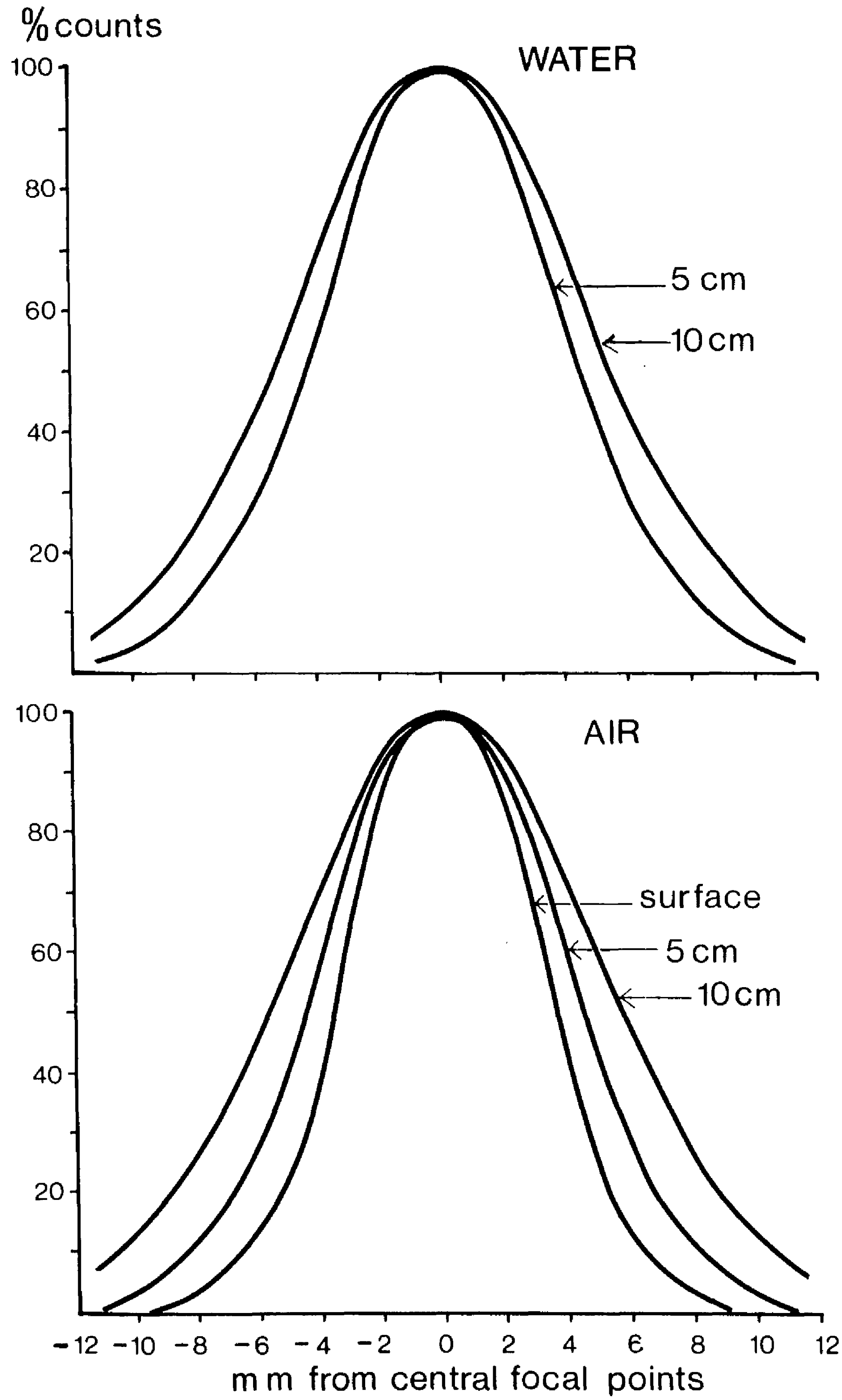

% counts
WATER
100
80
60
40
20
5 cm
10 cm
AIR
100
80
60
40
20
surface
5 cm
10 cm
−12 −10 −8 −6 −4 −2 0 2 4 6 8 10 12
m m from central focal points

Figure 16

Effect of smoothing and filtering on ^{99m}Tc point source at 10 cm from the High Resolution collimator.

^{99m}Tc point source at 10cm of the High Resolution collimator

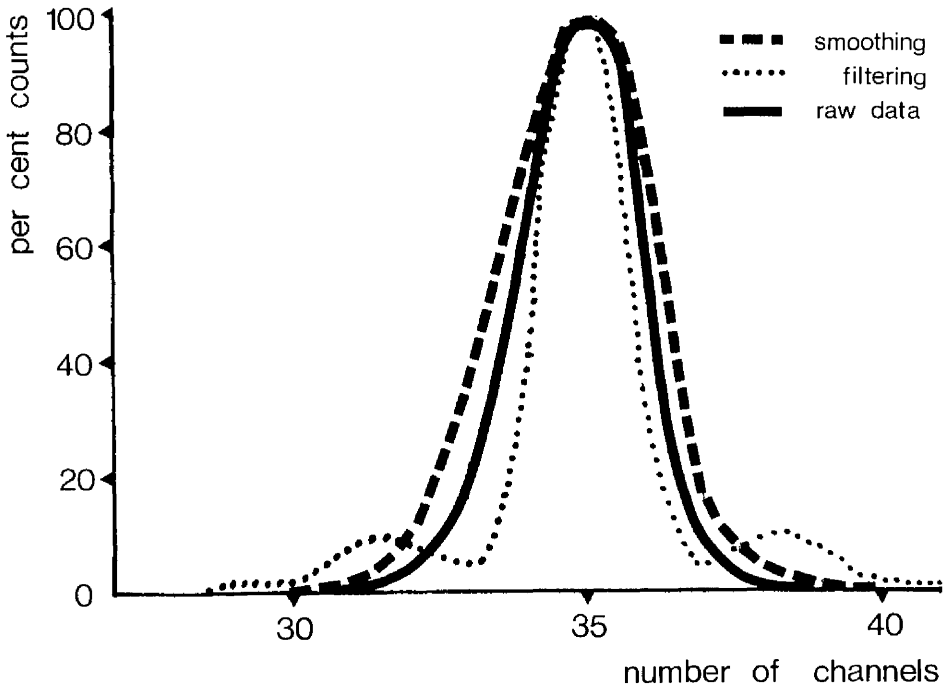

Figure 17

Black and white Polaroid of the Williams liver phantom on the High Resolution collimator

(a) at surface

(b) at 10 cm.

(a)

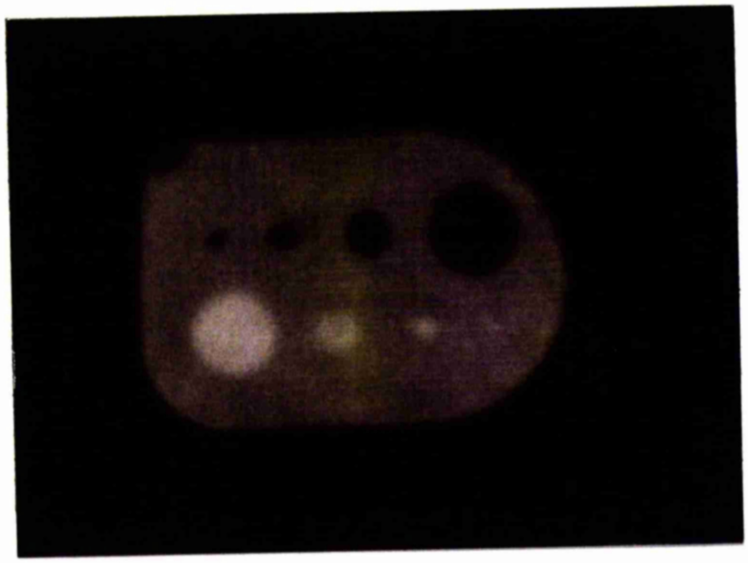

(b)

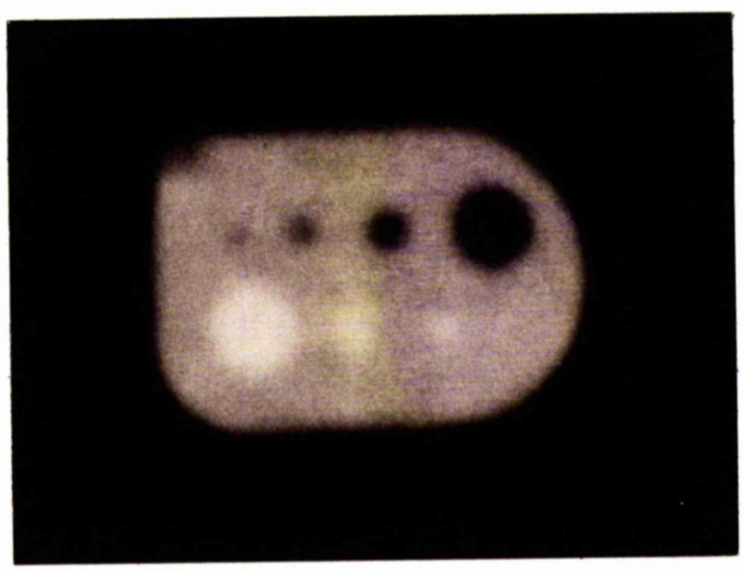

Figure 18

Profiles across the image of a Williams liver phantom at 10 cm from the High Resolution collimator

(a) cold spots

(b) hot spots.

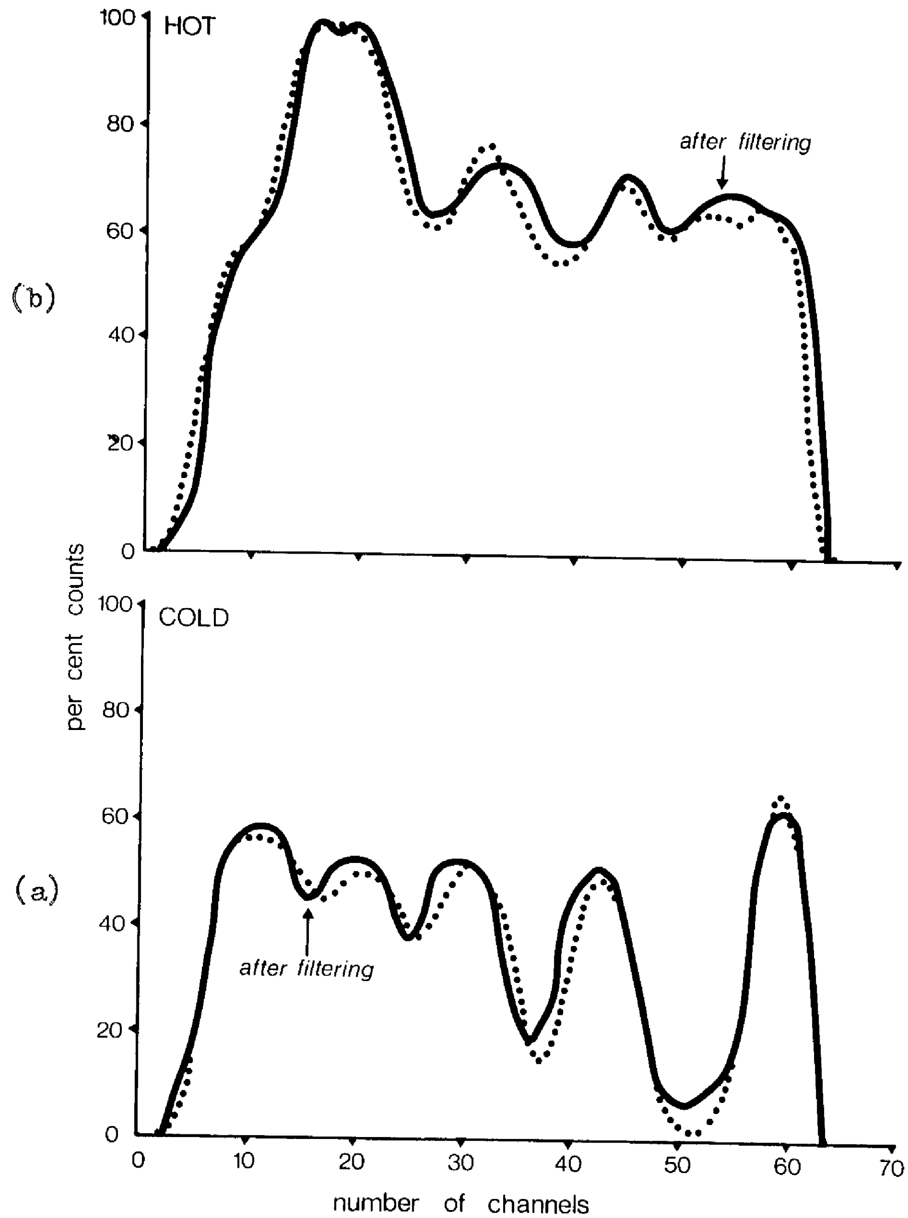

(b)
HOT
after filtering
100
80
60
40
20
0
(a)
COLD
after filtering
per cent counts
number of channels
0
10
20
30
40
50
60
70

Figure 19

Profiles across the image of a Williams liver phantom at surface and at 10 cm from the High Resolution collimator

(a) cold spots

(b) hot spots.

(a)

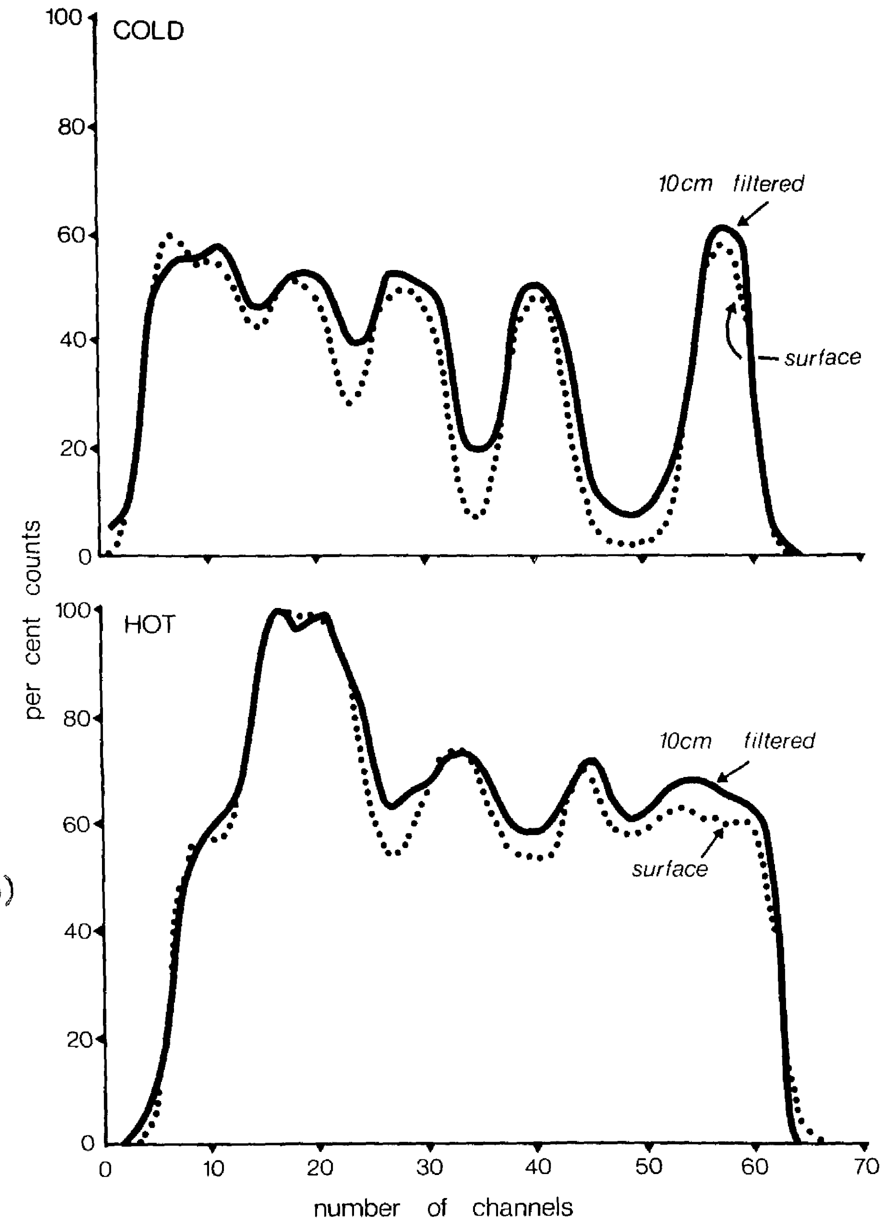

COLD
10cm filtered
surface
HOT
10cm filtered
surface
per cent counts
number of channels
0
10
20
30
40
50
60
70
0
20
40
60
80
100

(b)

Figure 20

Colour Polaroid picture of a Williams liver phantom before and after filtering at 10 cm.

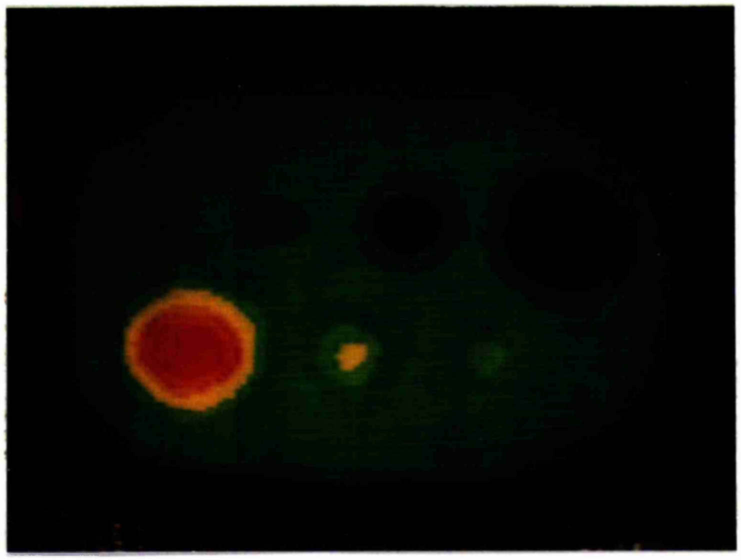

before

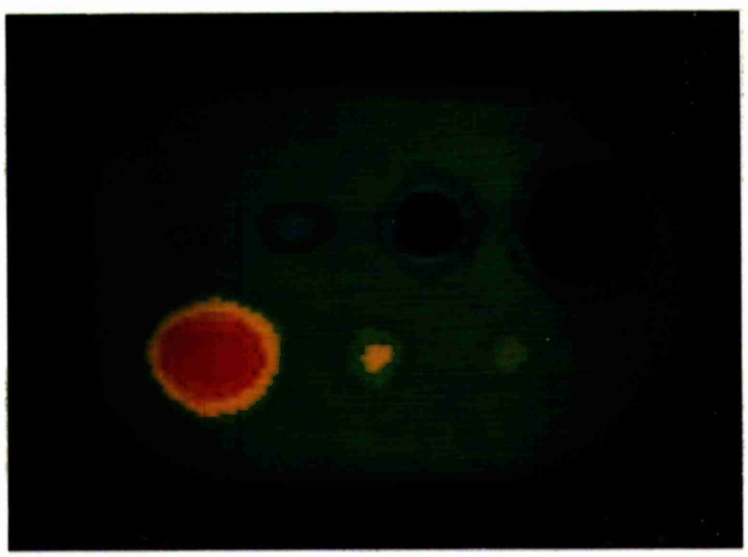

after

CHAPTER V

PHANTOM STUDIES

1. Liver Phantom

A liver phantom was made using a uniformity circular disc filled with ^{99m}Tc mixed with water. A sheet of lead cut to a liver shape at the middle was placed on top of this phantom. The edges of the cut-out were feathered to reduce the unnatural sharpness of the edge of the image. A number of pieces of lead, steel and aluminium of different sizes, shapes and thickness simulated lesions. A series of fifty pictures of raw data of this "liver" (5 cm away from the surface of the High Resolution collimator) was obtained with a preset count of 300,000, uniformed and recorded on the magnetic tape. There was one or no lesion for each picture. There were thirty pictures with lesions and twenty pictures without lesions. At the same time Polaroid pictures were taken for comparison with the pictures on the colour television.

Four methods of image display were chosen to apply to these raw data. The first and second methods are the raw data displayed by linear scale and the raw data displayed by statistical scale of plus or minus one standard deviation. The third and fourth methods are smoothing by a factor

$$\begin{bmatrix} 1 & 1 & 1 \\ 1 & 1 & 1 \\ 1 & 1 & 1 \end{bmatrix}$$

and the combination of smoothing plus filtering by a filter obtained from the appropriate distance from the collimator as in Chapter IV. These two methods are compared with the raw data displayed in a linear scale.

2. Assessment of Display Techniques

A group of eight people were asked to examine the pictures, both Polaroid and on colour television, by each method of display on different occasions. These people were familiar with the scintiscanning images. The pictures on the colour television were viewed at a distance of six to eight feet from the screen with the light on. The screen was one foot above eye level.

One of five levels of confidence of the presence of a lesion was marked by each person for each image. These five choices are "absent" (0-20%), "could be" (20-40%), "fifty-fifty" (40-60%), "probable" (60-80%) and "definite" (80-100%).

The process of examination is, firstly, looking through the whole series of the pictures once without making a choice, to familiarise the viewers with each type of display. On the second pass each picture was assigned to a certain level of confidence.

From the scores obtained from the observer, the Receiver Operating Characteristic Curves (R.O.C.) were plotted, using confidence rating procedure, as a percentage of true positive against percentage of false positive.

The following definitions were used:

$$\text{True positive (TP)} = \frac{\text{number of lesions correctly detected}}{\text{the number of phantoms with lesions}} \times 100$$

$$\text{False positive (FP)} = \frac{\text{number of lesions incorrectly detected}}{\text{the number of phantoms without lesions}} \times 100$$

$$\text{True negative (TN)} = \frac{\text{number of correct negatives}}{\text{the number of phantoms without lesions}} \times 100$$

$$\text{False negative (FN)} = \frac{\text{number of incorrect negatives}}{\text{the number of phantoms with lesions}} \times 100$$

$$\text{Therefore} \quad TP + FN = 100\%$$

$$\text{and} \quad TN + FP = 100\%$$

The R.O.C. curves were plotted for each observer and finally the total scores were plotted as the representative of the group for each mode of display.

Results and Discussion

From the study in this chapter, the plots of R.O.C. curves for each observer are shown in Figure 21. Seven of the observers show the same pattern of curves. Observer F produced a very unusual set of results. Therefore, two types of total scores (Tables 4, 5, 6, 7, 8 and 9) were plotted as seen in Figure 22a and Figure 22b for eight and seven observers respectively. Each method has four confidence levels, so each curve contains four points plotted as percentage true positive against percentage false positive. The confidence level "absent" (0-20%) for each method was plotted (Figure 23) as a complementary result to Figures 22a and 22b.

The results show that the response of the observers to colour television is better than Polaroid at all levels of confidence either individual or total scores, except observer F. At the confidence level "definite" (80-100%) the percentage of true positive and false positive for Polaroid and colour television, raw data displayed in linear scale are 27/1 and 43/2. If the process of smoothing and smoothing plus filtering were applied, the detectability is improved to 63/3 and 69/2 respectively. The raw data displayed by a statistical scale of plus or minus one standard deviation is poorer than by linear scale. This is because the upper bands of the statistical scale of plus or minus one standard deviation are wider than the linear scale for the count levels in these images (Table 10), whereas those of plus or minus half a standard deviation are similar to the linear scale. This causes the changes in colour to be insufficient to detect the smaller changes in count rate. Some pictures of "liver" phantom at each mode of display are shown in Figure 24.

Some examples of clinical data using the statistical colour scale with a narrower bandwidth of plus or minus half a standard deviation plus smoothing are shown in Figure 25.

All currently available scintillation cameras have at least one cathode-ray tube that has a phosphor suitable for use with Polaroid camera. Polaroid film has a relatively narrow dynamic contrast range and limited grey scale, which is the disadvantage of Polaroid compared with colour display.

Colour scanning is popular with some physicians and it appears easier to interpret patterns of different colours ranging from blue to red, than varying shades of grey; in addition colours allow a semiquantitative interpretation of the count density (Hine and Erickson, 1974).

At the present time, no image processing technique has been proved by careful statistical study on clinical scintigrams to improve the diagnostic ability of nuclear medicine procedures (Pizer et al, 1974).

In the present study, the "liver" phantom was designed to produce a good simulation of the image of the real liver. The lesion was, therefore, a cold spot on a hot background and the results do not necessarily apply to a hot spot on a cold background, such as a bone scan. Its main deficiency was having uniform activity distribution rather than the activity profile typical of a real liver. However, the number of counts recorded is typical of a real study, so the statistical nature of the image was similar. The improvement of these phantom images by various display techniques indicate that real images would also benefit in a similar way (Figure 25).

The processed images of the phantom by smoothing and filtering give better presentation to the human observers than the raw data. If the principal degradation of the image is noise it is often significantly improved by smoothing and it does show that a small amount of filtering combined with smoothing will increase the resolution effectively in some scintigrams. At the same time quite often it increases artefacts as well. Filtering tends to emphasize both real structures and noise artefacts. This tendency must be taken into account when interpreting the images and the diagnosis can be made only after adequate training for each physician for each technique.

Table 4. <u>Polaroid.</u> <u>Percentage Visual Response of a set of Observers Using Confidence Rating Procedure</u>

Confidence Level		Cumulative number of lesions detected for each observer A	B	C	D	E	G	H	Cumulative number of lesions detected for 7 observers	Cumulative percentage of TP and FP respectively	Observer F	Cumulative total for 8 observers	Cumulative percentage of TP and FP respectively
"Definite"	TP	6	8	5	4	9	6	4	42	20	22	64	27
80-100%	FP	0	0	0	0	0	0	0	0	0	2	2	1
"Probable"	TP	8	17	9	11	15	9	7	76	36	25	101	42
60-80%	FP	0	4	0	0	1	2	0	7	5	4	11	7
"Fifty-fifty"	TP	10	23	14	16	20	15	8	106	50	26	132	55
40-60%	FP	0	9	4	2	5	3	0	23	16	5	28	18
"Could be"	TP	18	28	25	25	27	23	13	159	76	28	187	78
20-40%	FP	1	13	12	10	13	10	1	60	43	9	69	43

Table 5. <u>Colour Television Display, Linear Scale, Raw Data.</u> <u>Percentage Visual</u>

<u>Response of a set of Observers Using Confidence Rating Procedure</u>

Confidence Level		Cumulative number of lesions detected for each observer A	B	C	D	E	G	H	Cumulative number of lesions detected for 7 observers	Cumulative percentage of TP and FP respectively	Observer F	Cumulative total for 8 observers	Cumulative percentage of TP and FP respectively
"Definite"	TP	14	11	7	11	14	21	5	83	40	20	103	43
80-100%	FP	0	0	0	0	0	0	0	0	0	3	3	2
"Probable"	TP	16	24	15	21	24	21	9	130	62	21	151	63
60-80%	FP	0	0	0	0	0	0	0	0	0	5	5	3
"Fifty-fifty"	TP	17	26	23	25	26	24	12	153	73	21	174	73
40-60%	FP	0	1	2	0	5	2	0	10	7	6	16	10
"Could be"	TP	22	29	26	28	26	29	20	180	86	22	202	84
20-40%	FP	1	9	6	9	9	7	0	41	29	7	48	30

Table 6. <u>Colour Television Display, Statistical Scale plus or minus One Standard Deviation.</u>

<u>Percentage Visual Response of a set of Observers Using Confidence Rating Procedure</u>

Confidence Level		Cumulative number of lesions detected for each observer							Cumulative number of lesions detected for 7 observers	Cumulative percentage of TP and FP respectively	Observer F	Cumulative total for 8 observers	Cumulative percentage of TP and FP respectively
		A	B	C	D	E	G	H					
"Definite"	TP	10	3	7	13	16	13	16	78	37	21	99	41
80-100%	FP	0	0	0	0	0	0	0	0	0	4	4	3
"Probable"	TP	14	12	8	19	20	21	18	112	53	21	133	55
60-80%	FP	1	0	0	1	1	0	0	3	2	4	7	4
"Fifty-fifty"	TP	16	19	12	21	24	25	20	137	65	21	158	66
40-60%	FP	1	0	0	2	5	2	0	10	7	5	15	9
"Could be"	TP	22	25	20	24	27	29	22	169	80	21	190	79
20-40%	FP	1	3	0	5	9	9	2	29	21	5	34	21

Table 7. Colour Television Display, Linear Scale, Smoothing. Percentage Visual Response of a set of Observers Using Confidence Rating Procedure

Confidence Level		Cumulative number of lesions detected for each observer A	B	C	D	E	G	H	Cumulative number of lesions detected for 7 observers	Cumulative percentage of TP and FP respectively	Observer F	Cumulative total for 8 observers	Cumulative percentage of TP and FP respectively
"Definite"	TP	20	10	19	17	22	21	16	125	60	27	152	63
80-100%	FP	0	0	0	0	0	0	0	0	0	5	5	3
"Probable"	TP	23	21	23	23	24	24	17	155	74	27	182	76
60-80%	FP	0	0	0	0	1	0	0	1	1	5	6	4
"Fifty-fifty"	TP	24	26	26	25	24	25	23	173	82	27	200	83
40-60%	FP	0	2	1	0	1	1	0	5	4	5	10	6
"Could be"	TP	25	27	26	26	24	27	24	179	85	27	206	86
20-40%	FP	1	7	1	1	3	1	1	15	11	7	22	14

Table 8. Colour Television Display, Linear Scale, Smoothing plus Filtering. Percentage

Visual Response of a set of Observers Using Confidence Rating Procedure

Confidence Level		Cumulative number of lesions detected for each observer							Cumulative number of lesions detected for 7 observers	Cumulative percentage of TP and FP respectively	Observer	Cumulative total for 8 observers	Cumulative percentage of TP and FP respectively
		A	B	C	D	E	G	H			F		
"Definite"	TP	20	12	20	21	26	23	23	145	72	28	173	69
80-100%	FP	0	1	0	0	2	0	0	3	3	2	5	2
"Probable"	TP	25	24	24	25	26	27	25	176	85	28	204	84
60-80%	FP	0	2	1	1	2	0	1	7	6	2	9	5
"Fifty-fifty"	TP	25	27	27	27	26	27	25	184	88	28	212	88
40-60%	FP	0	2	2	1	2	2	1	10	8	2	12	7
"Could be"	TP	26	29	27	27	27	29	26	191	91	28	219	91
20-40%	FP	2	4	2	2	2	2	2	16	11	2	18	11

Table 9. <u>Percentage of True Negative Against False Negative</u>

<u>For Each Method of Image Processing</u>

Method		Cumulative number of lesions detected for each observer A	B	C	D	E	G	H	Cumulative number of lesions detected for 7 observers	Cumulative percentage of TN and FN respectively	Observer F	Cumulative total for 8 observers	Cumulative percentage of TN and FN respectively
Polaroid	TN	19	7	8	10	7	10	19	80	57	11	91	57
	FN	12	2	5	5	3	7	17	51	24	2	53	22
T.V., linear scale	TN	19	11	14	11	11	13	20	99	71	13	112	70
Raw data	FN	8	1	4	2	4	1	10	30	14	8	38	16
T.V., statistical scale ($\pm$ 1 S.D.)	TN	19	17	20	15	11	11	18	111	79	15	126	79
Raw data	FN	8	5	10	6	3	1	8	41	20	9	50	21
T.V., linear scale	TN	19	13	19	19	17	19	19	125	89	13	138	86
Smoothing	FN	5	3	4	4	6	3	6	31	15	3	34	14
T.V., linear scale	TN	18	16	18	18	18	18	18	124	89	18	142	89
Smoothing plus filtering	FN	4	1	3	3	3	1	4	19	9	2	21	9

Table 10. Comparison of Fifteen Levels of Linear Scale and Statistical Scale from one of the "Liver" Phantom

Linear scale	Statistical scale $\pm$ 1 S.D.	Statistical scale $\pm \frac{1}{2}$ S.D.
363	363	363
340	326	345
316	291	328
292	258	311
268	227	295
244	198	279
220	171	264
196	146	249
172	123	235
148	102	221
124	83	208
100	66	195
76	51	183
52	38	171
28	27	159

Figure 21

The R.O.C. curves for each observer. Percentage true positive against percentage false positive.

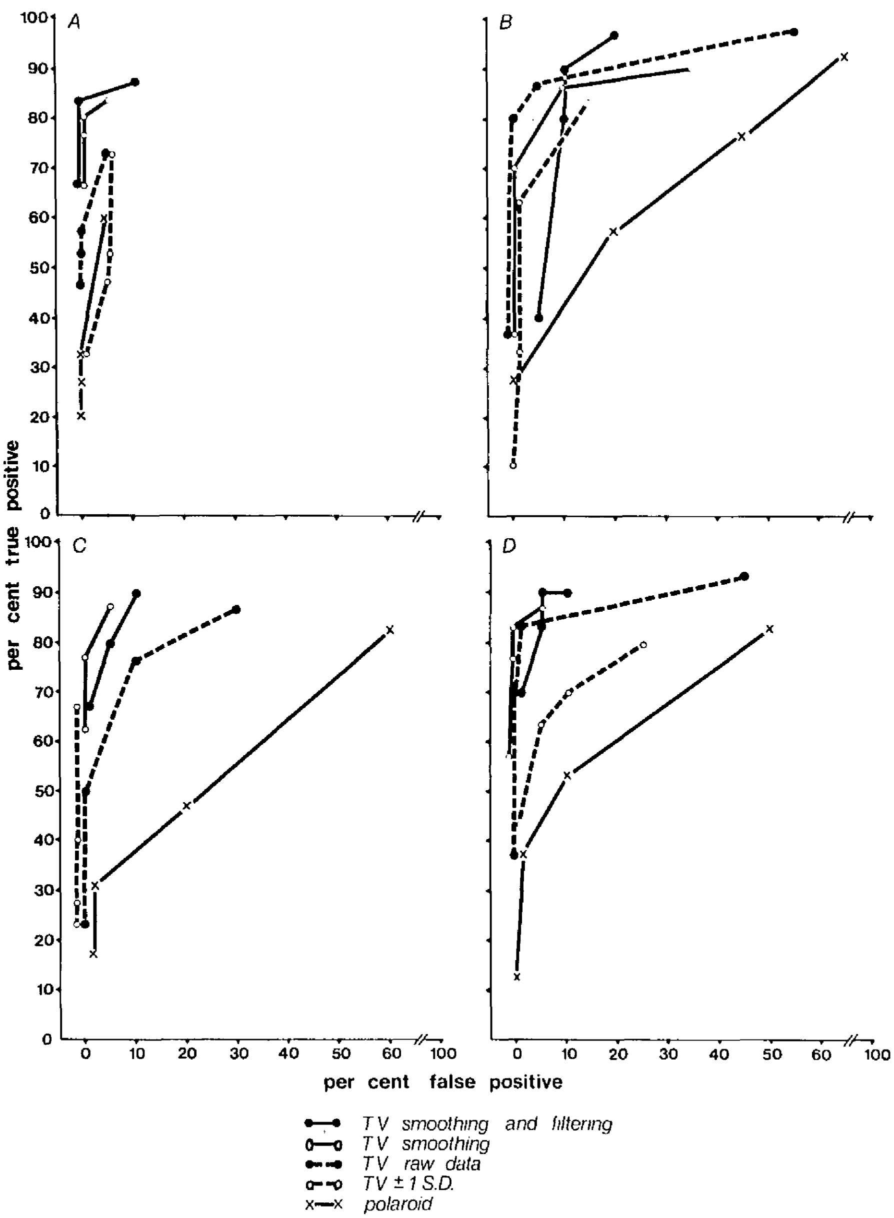

A
B
C
D
per cent true positive
per cent false positive
TV smoothing and filtering
TV smoothing
TV raw data
TV ± 1 S.D.
polaroid

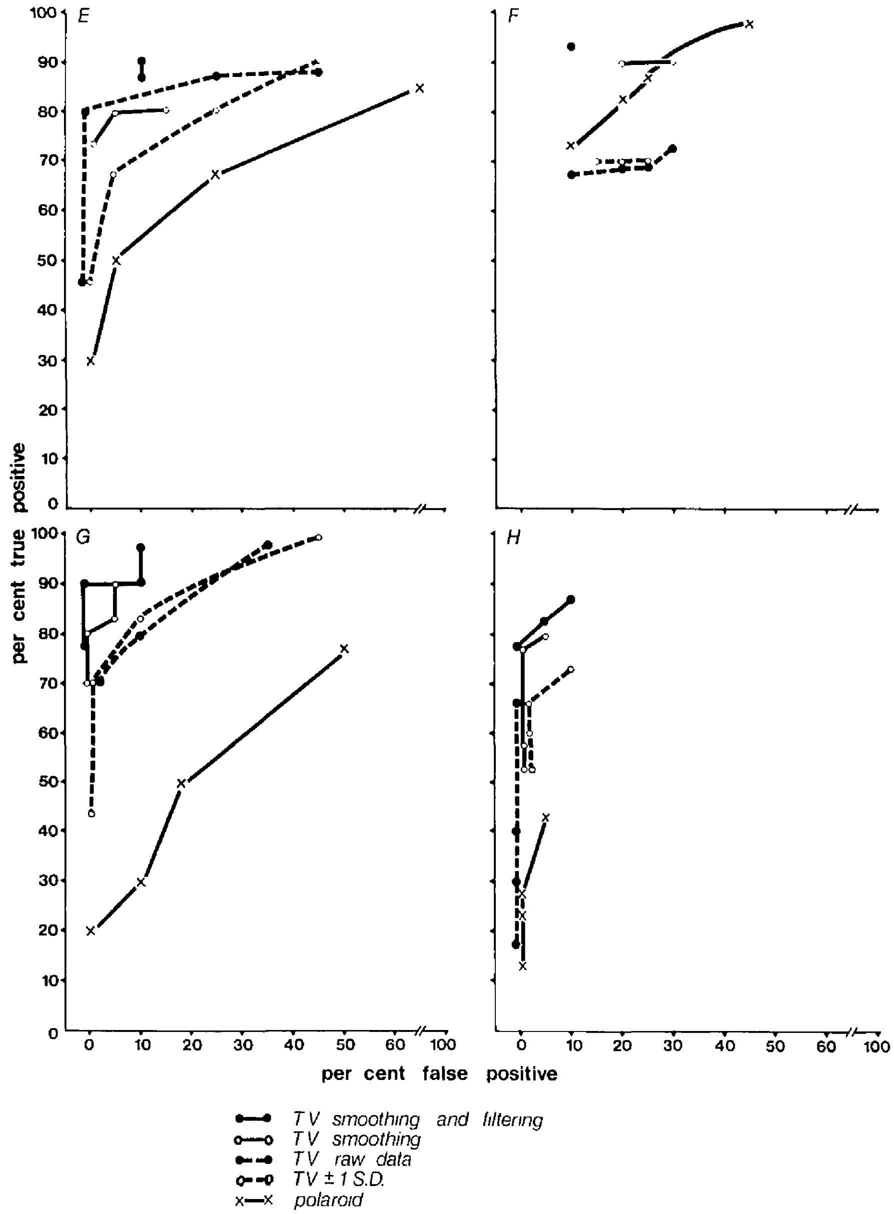
E
F
G
H
per cent true positive
per cent false positive
TV smoothing and filtering
TV smoothing
TV raw data
TV ± 1 S.D.
polaroid

Figure 22

(a) The R.O.C. curves for eight observers.

(b) The R.O.C. curves for seven observers.

Percentage true positive against false positive.

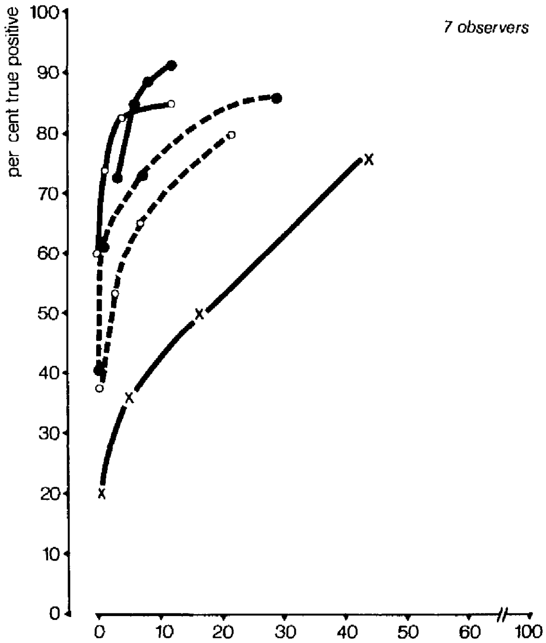

per cent true positive
7 observers
0
10
20
30
40
50
60
70
80
90
100
0
10
20
30
40
50
60
100

(b)

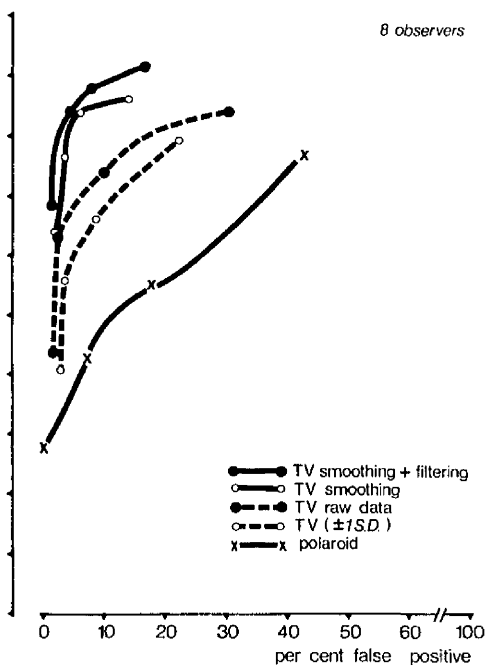

8 observers
TV smoothing + filtering
TV smoothing
TV raw data
TV (±1S.D.)
polaroid
0
10
20
30
40
50
60
100
per cent false positive

(a)

Figure 23

Percentage true negative against false negative for each method of image processing.

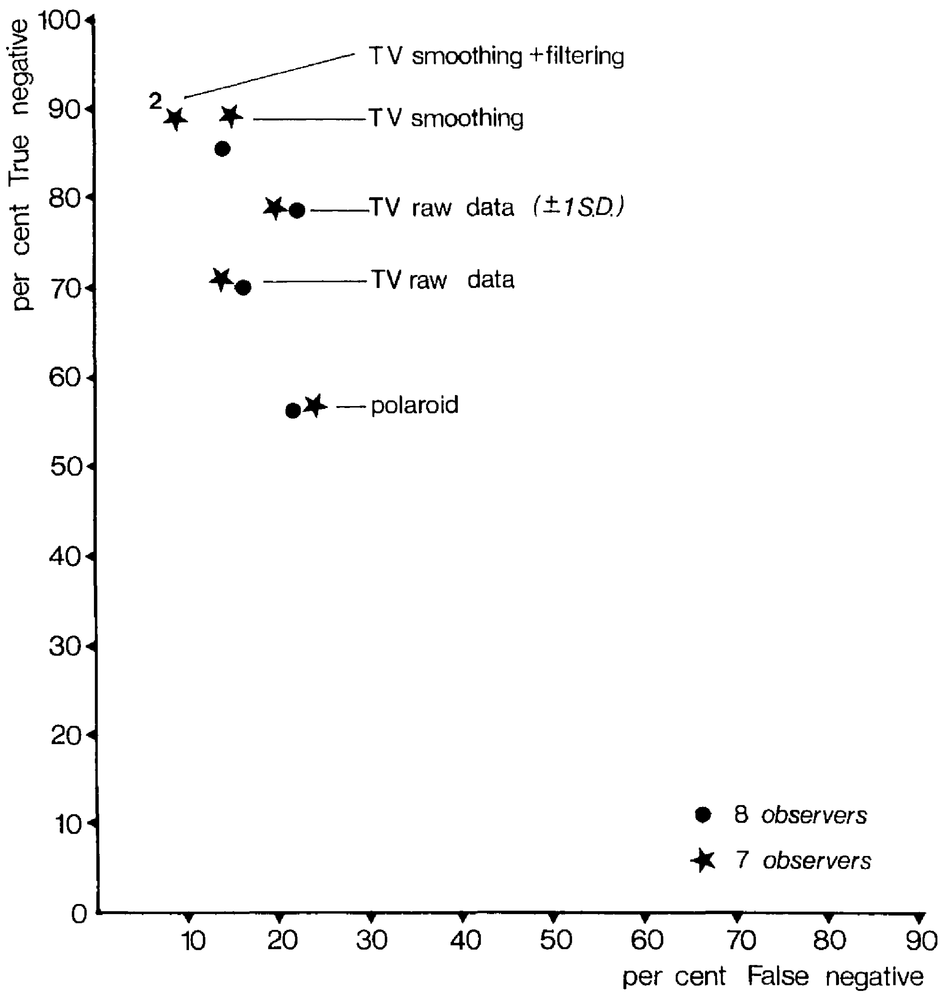

per cent True negative
100
90
80
70
60
50
40
30
20
10
0
TV smoothing +filtering
2
TV smoothing
TV raw data (±1 S.D.)
TV raw data
polaroid
8 observers
7 observers
10
20
30
40
50
60
70
80
90
per cent False negative

<u>Figure 24</u>

Pictures of the "liver" phantom

(a) Polaroid.

(b) Colour television, raw data, linear scale.

(c) Colour television, raw data, plus or minus one standard deviation.

(d) Colour television, raw data, plus or minus half a standard deviation.

(e) Colour television, smoothed, linear scale.

(f) Colour television, smoothing plus filtering, linear scale.

(a)

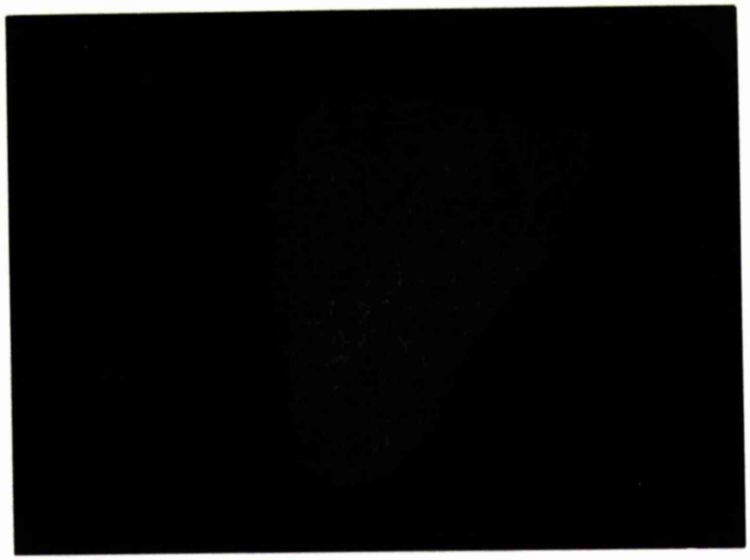

(b)

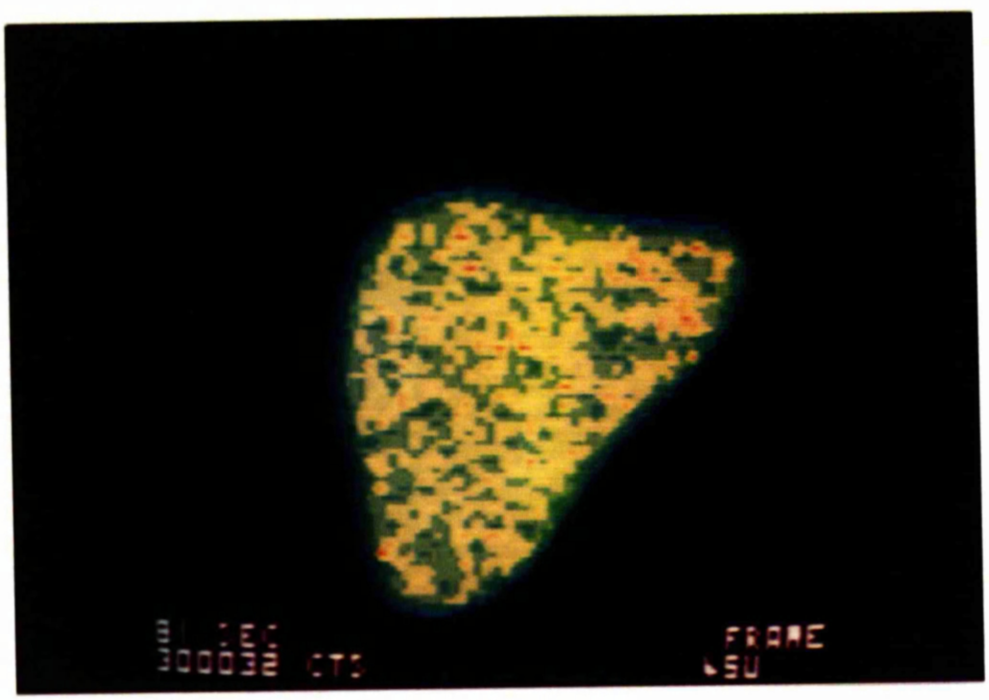

(c)

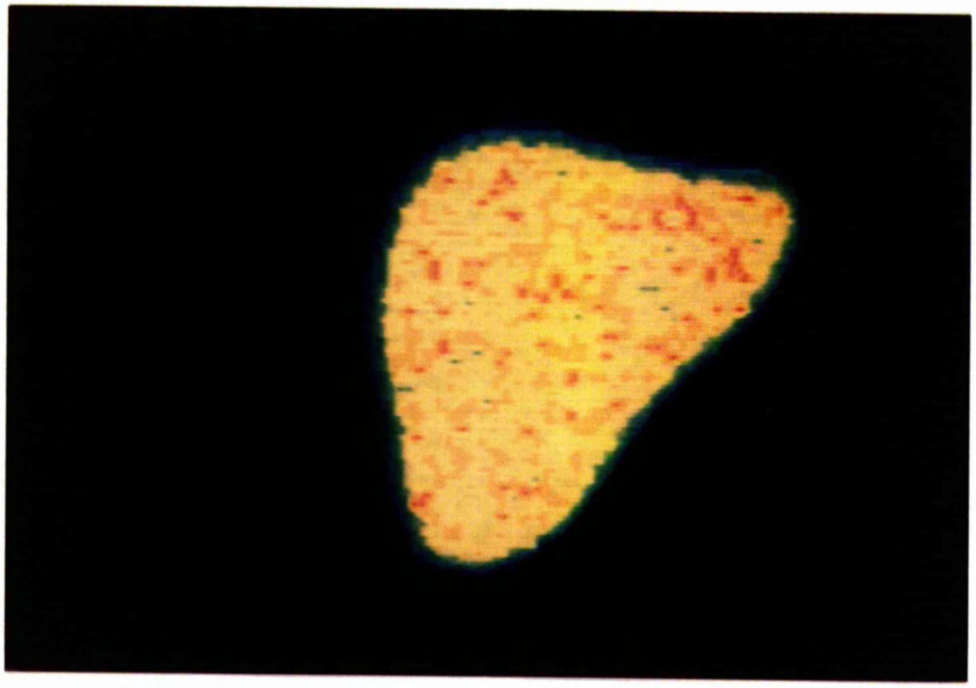

(d)

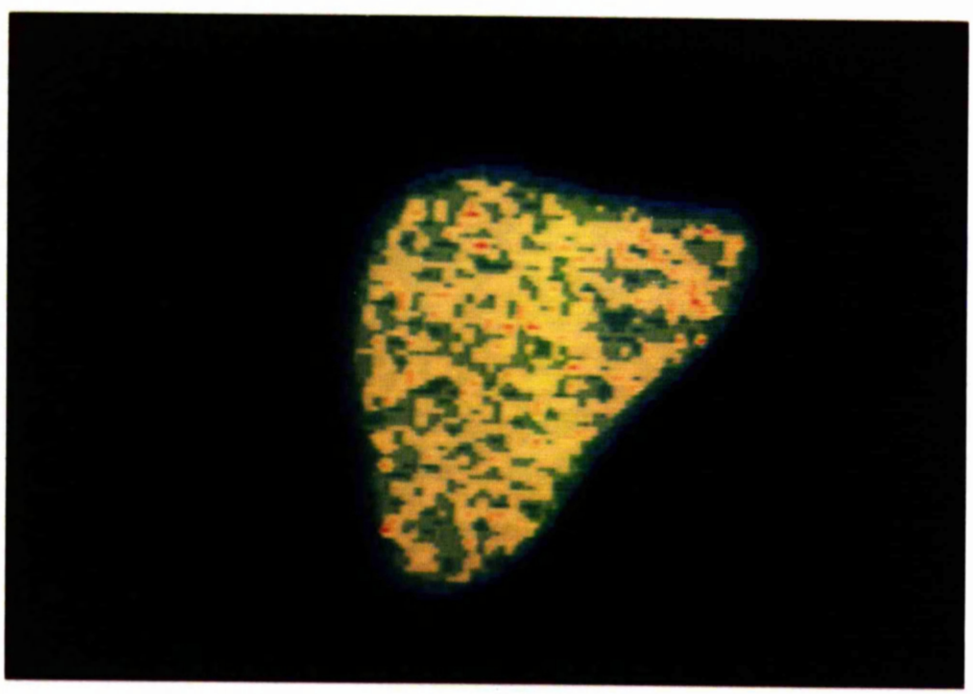

(e)

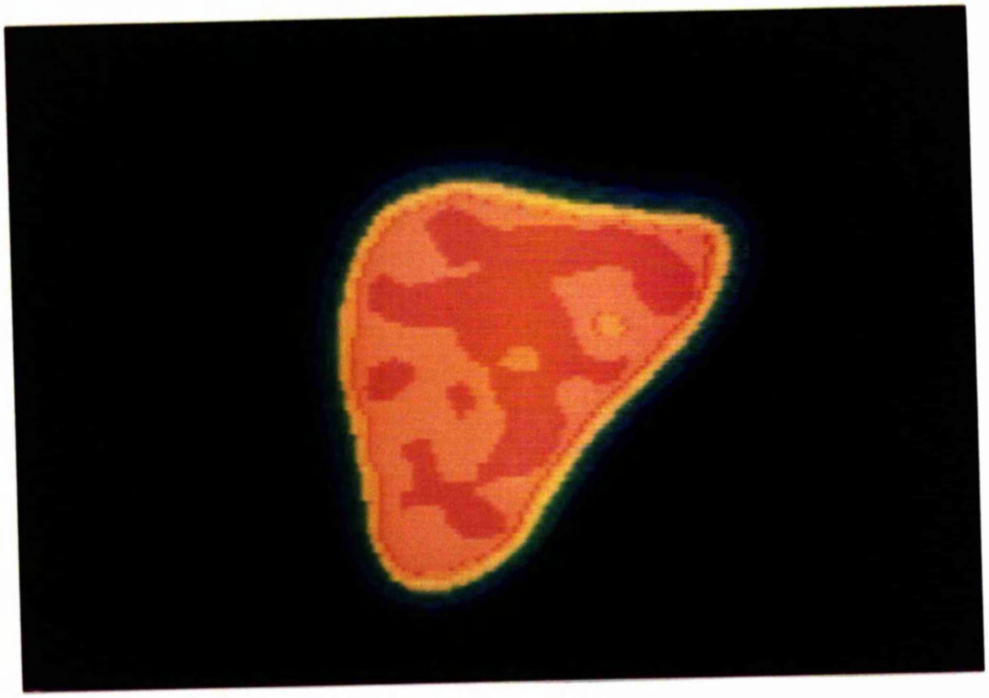

(f)

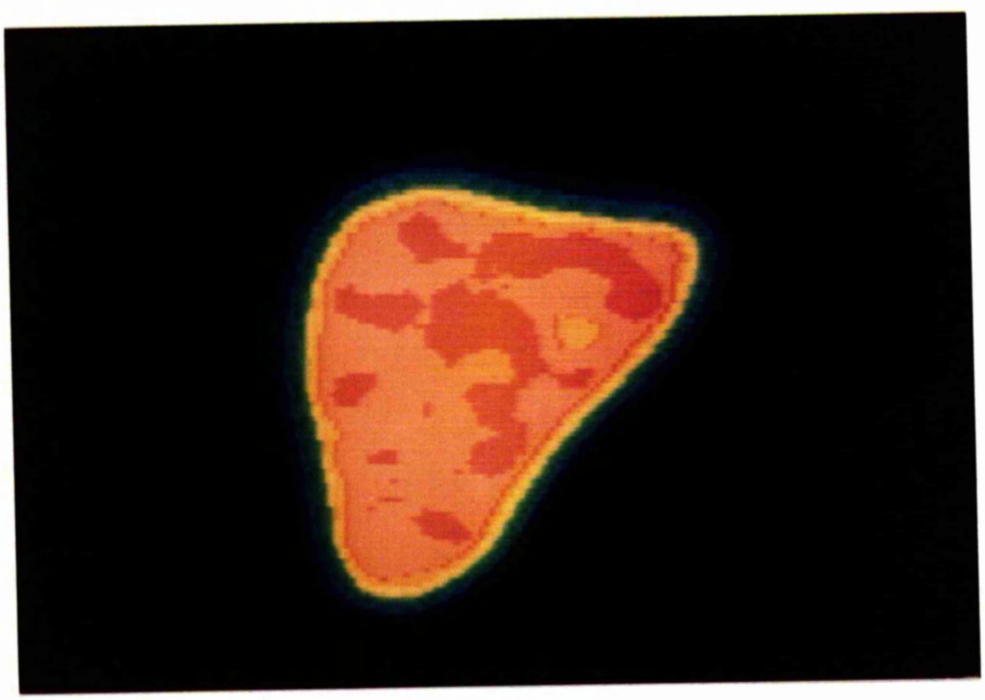

Figure 25

Clinical pictures displayed by statistical scale plus or minus half a standard deviation

(a) Bone scan. Rib before and after smoothing.

(b) Skull before and after smoothing.

(c) Liver scan. Lateral view of a liver before and after smoothing.

(a)

before

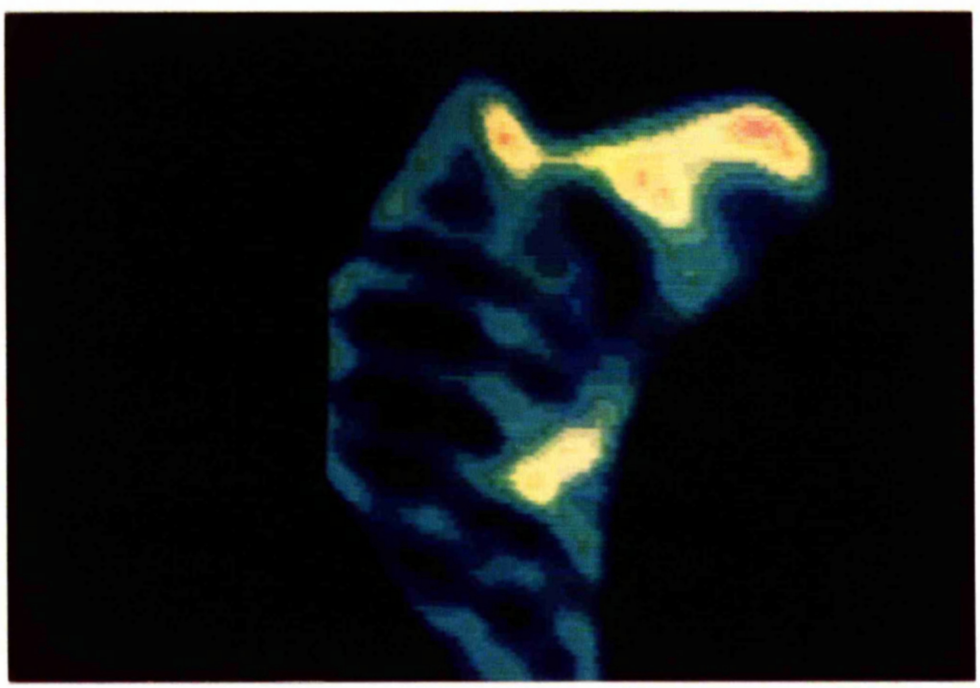

after

(b)

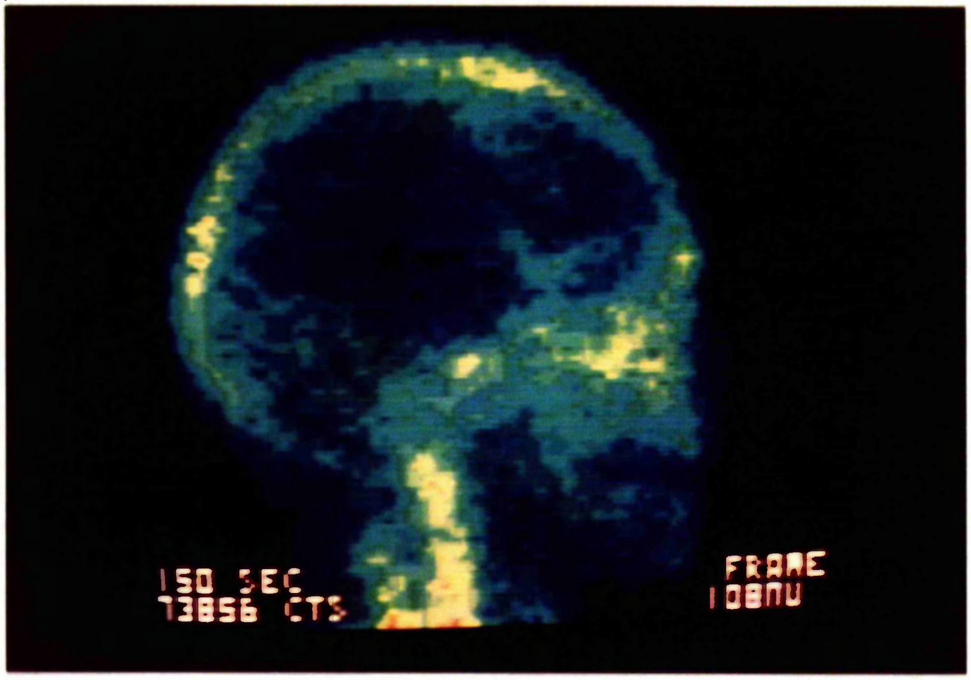

before

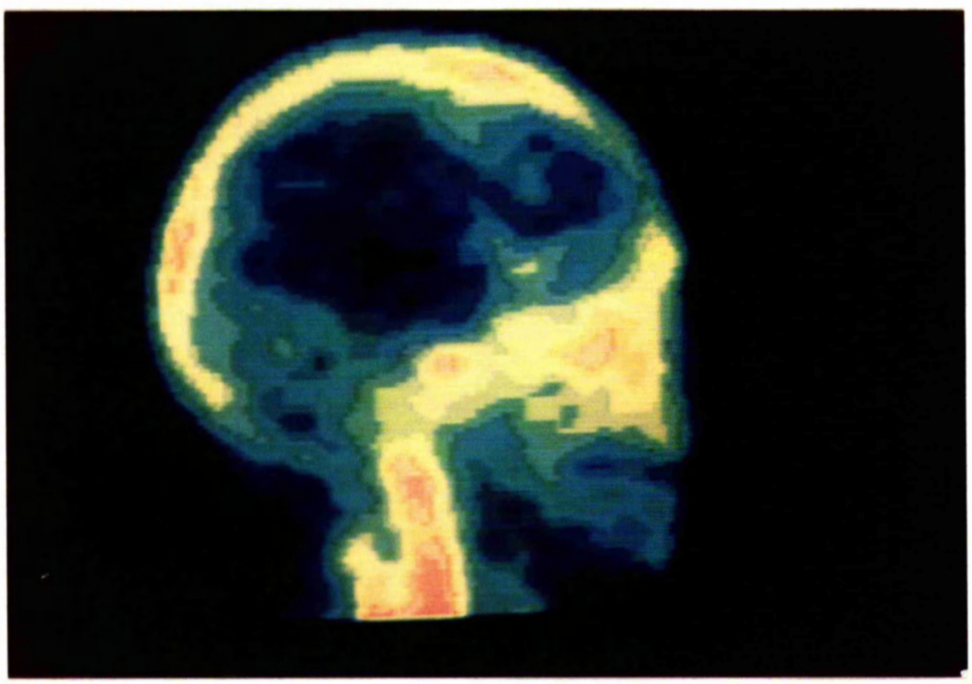

after

(c)

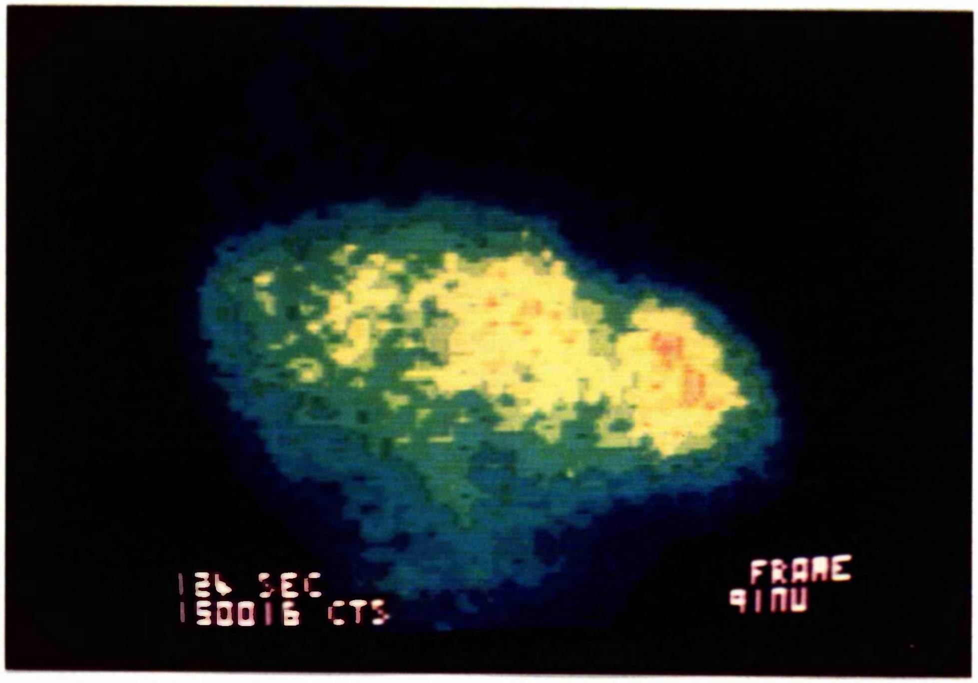

before

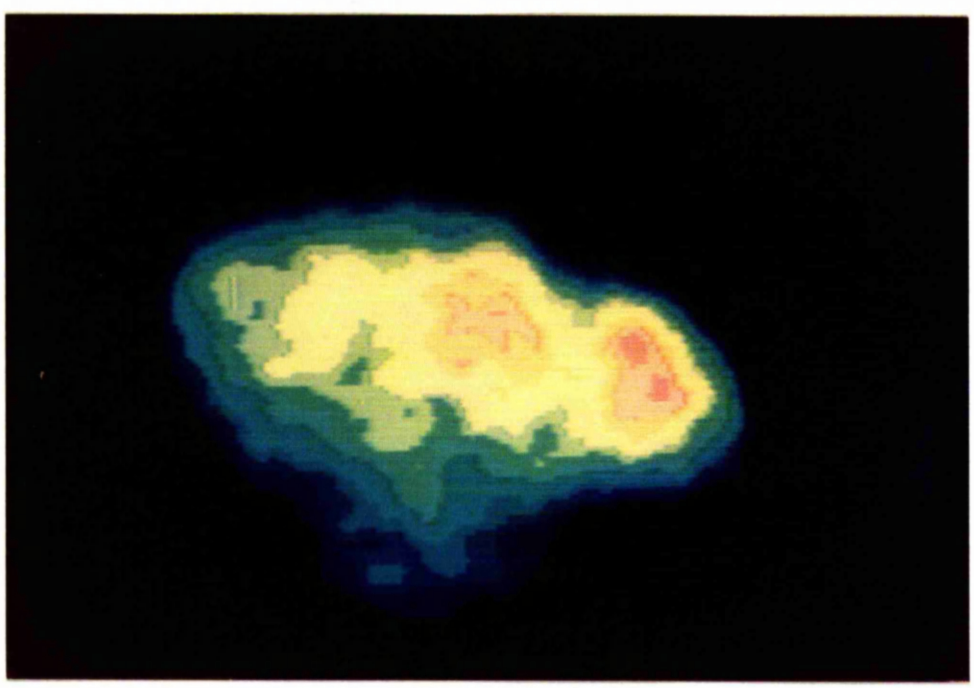

after

APPENDIX 1

IMAGE PROCESSING PROGRAM

```
FMAX ,EQU  ,02200
DISP ,EQU  ,01727
MAXM ,EQU  ,02231
MINM ,EQU  ,02232
LTØR ,BEGI ,03153
     ,ØRG  ,0775
     ,SUB  ,='J'
     ,JAZ  ,030000
     ,ØRG  ,030000
     ,EXC  ,0540
     ,CALL ,INPU
     ,LRLA ,8
     ,STA  ,KEEP
     ,CALL ,INPU
     ,ØRA  ,KEEP
     ,STA  ,KEEP
     ,SUB  ,='GC'
     ,JAZ  ,1
     ,LDA  ,KEEP
     ,SUB  ,='A2'
     ,JAZ  ,036000
     ,LDA  ,KEEP
     ,SUB  ,='NP'
     ,JAZ  ,NINE
     ,LDA  ,KEEP
     ,SUB  ,='CE'
     ,JAZ  ,SEE
     ,LDA  ,KEEP
     ,SUB  ,='TF'
     ,JAZ  ,TFPF
     ,JMP  ,030000
NINE ,CALL ,NP
     ,CALL ,EXCH
     ,JMP  ,SEE
NP   ,ENTR ,
     ,LDA  ,FLAX
     ,JAN  ,*+9
     ,LDA  ,AØNE
     ,ADD  ,ATWØ
     ,ASLA ,2
     ,ADD  ,AZER
     ,STA  ,KEEP+2
     ,JMP  ,*+4
     ,LDA  ,DIVR
     ,STA  ,KEEP+2
     ,LDX  ,=010000
STRT ,TXA  ,
     ,SUB  ,=010100
     ,JAN  ,NEW1
     ,TXA  ,
```

```
        ,SUB    ,=017700
        ,JAP    ,NEW1
        ,TXA    ,
        ,ANA    ,=000077
        ,JAZ    ,NEW1
        ,SUB    ,=000077
        ,JAZ    ,NEW1
        ,TZA    ,
        ,LDB    ,0,1
        ,MUL    ,AZER
        ,STA    ,KEEP
        ,STB    ,KEEP+1
        ,CALL   ,ADD,63,65,-63,-65,0
        ,CALL   ,MUL,ATWØ
        ,LDA    ,ATWØ
        ,JAN    ,*+6
        ,CALL   ,DPAD
        ,JMP    ,*+4
        ,CALL   ,DSUB
        ,CALL   ,ADD,1,64,-1,-64,0
        ,CALL   ,MUL,AØNE
        ,LDA    ,AØNE
        ,JAN    ,*+6
        ,CALL   ,DPAD
        ,JMP    ,*+4
        ,CALL   ,DSUB
        ,LDA    ,KEEP
        ,JAN    ,NEW1
        ,LDB    ,KEEP+1
        ,DIV    ,KEEP+2
        ,JØF    ,*+4
        ,JMP    ,*+3
        ,LDB    ,=077777
        ,STBE   ,010000,1
        ,JMP    ,*+5
NEW1    ,TZA    ,
        ,STAE   ,010000,1
        ,TXA    ,
        ,SUB    ,=017777
        ,JAZ    ,*+5
        ,IXR    ,
        ,JMP    ,STRT
        ,JMP*   ,NP
TFPF    ,CALL   ,TF
        ,CALL   ,EXCH
        ,JMP    ,SEE
TF      ,ENTR   ,
        ,LDA    ,FLAG
        ,JAN    ,*+13
        ,LDA    ,KØNE
```

```
     ,ADD    ,KTWØ
     ,ADD    ,KTRE
     ,ADD    ,KFØR
     ,ADD    ,KFØR
     ,ADD    ,KFIV
     ,ASLA   ,2
     ,ADD    ,KZER
     ,STA    ,KEEP+2
     ,JMP    ,*+4
     ,LDA    ,DIVR
     ,STA    ,KEEP+2
     ,LDX    ,=010000
TF1  ,TXA    ,
     ,SUB    ,=010200
     ,JAN    ,NEW2
     ,TXA    ,
     ,SUB    ,=017600
     ,JAP    ,NEW2
     ,TXA    ,
     ,ANA    ,=000076
     ,JAZ    ,NEW2
     ,SUB    ,=000076
     ,JAZ    ,NEW2
     ,TZA    ,
     ,LDB    ,0,1
     ,MUL    ,KZER
     ,STA    ,KEEP
     ,STB    ,KEEP+1
     ,CALL   ,ADD,1,64,-1,-64,0
     ,CALL   ,MUL,KØNE
     ,LDA    ,KØNE
     ,JAN    ,*+6
     ,CALL   ,DPAD
     ,JMP    ,*+4
     ,CALL   ,DSUB
     ,CALL   ,ADD,65,63,-65,-63,0
     ,CALL   ,MUL,KTWØ
     ,LDA    ,KTWØ
     ,JAN    ,*+6
     ,CALL   ,DPAD
     ,JMP    ,*+4
     ,CALL   ,DSUB
     ,CALL   ,ADD,2,128,-2,-128,0
     ,CALL   ,MUL,KTRE
     ,LDA    ,KTRE
     ,JAN    ,*+6
     ,CALL   ,DPAD
     ,JMP    ,*+4
     ,CALL   ,DSUB
     ,CALL   ,ADD,66,129,-66,-129,62,127,-62,-127,(
```

```
      ,CALL   ,MUL,KFØR
      ,LDA    ,KFØR
      ,JAN    ,*+6
      ,CALL   ,DPAD
      ,JMP    ,*+4
      ,CALL   ,DSUB
      ,CALL   ,ADD,126,130,-126,-130,0
      ,CALL   ,MUL,KFIV
      ,LDA    ,KFIV
      ,JAN    ,*+6
      ,CALL   ,DPAD
      ,JMP    ,*+4
      ,CALL   ,DSUB
      ,LDA    ,KEEP
      ,JAN    ,NEW2
      ,LDB    ,KEEP+1
      ,DIV    ,KEEP+2
      ,JØF    ,*+4
      ,JMP    ,*+3
      ,LDB    ,=077777
      ,STBE   ,010000,1
      ,JMP    ,*+5
NEW2  ,TZA    ,
      ,STAE   ,010000,1
      ,TXA    ,
      ,SUB    ,=017777
      ,JAZ*   ,TF
      ,IXR    ,
      ,JMP    ,TF1
      ,JMP*   ,TF
EXCH  ,ENTR   ,
      ,LDXI   ,-010000
      ,LDAE   ,020000,1
      ,LDBE   ,030000,1
      ,STAE   ,030000,1
      ,STBE   ,020000,1
      ,IXR    ,
      ,JXZ    ,*+4
      ,JMP    ,EXCH+3
      ,JMP*   ,EXCH
ADD   ,ENTR   ,
      ,TZA    ,
      ,LDBE*  ,ADD
      ,JBZ    ,*+10
      ,STBE   ,*+3
      ,ADDE   ,0,1
      ,INRE   ,ADD
      ,JMP    ,*-10
      ,INRE   ,ADD
      ,JMP*   ,ADD
```

```
MUL   ,ENTR   ,
      ,STA    ,KEEP+5
      ,LDBE*  ,MUL
      ,LDA    ,0,2
      ,JAP    ,*+4
      ,CPA    ,
      ,IAR    ,
      ,STAE   ,*+5
      ,TZA    ,
      ,LDB    ,KEEP+5
      ,MULI   ,0
      ,STA    ,KEEP+3
      ,STB    ,KEEP+4
      ,INRE   ,MUL
      ,JMP*   ,MUL
DPAD  ,ENTR   ,
      ,LDA    ,KEEP
      ,ADD    ,KEEP+3
      ,STA    ,KEEP
      ,LDA    ,KEEP+1
      ,ADD    ,KEEP+4
      ,JAP    ,*+5
      ,RØF    ,
      ,INR    ,KEEP
      ,ANA    ,=077777
      ,STA    ,KEEP+1
      ,JMP*   ,DPAD
DSUB  ,ENTR   ,
      ,LDA    ,KEEP
      ,SUB    ,KEEP+3
      ,STA    ,KEEP
      ,LDA    ,KEEP+1
      ,SUB    ,KEEP+4
      ,JAP    ,*+4
      ,JMP    ,*+5
      ,STA    ,KEEP+1
      ,JMP*   ,DSUB
      ,LRLA   ,1
      ,LSRA   ,1
      ,STA    ,KEEP+1
      ,LDA    ,KEEP
      ,DAR    ,
      ,STA    ,KEEP
      ,JMP*   ,DSUB
KEEP  ,BSS    ,6
INPU  ,ENTR   ,
      ,EXC    ,0440
      ,SEN    ,0201,*+5
      ,NØP    ,
      ,JMP    ,*-3
```

```
      ,CIA   ,01
      ,SEN   ,0101,*+5
      ,NØP   ,
      ,JMP   ,*-3
      ,ØAR   ,01
      ,JMP*  ,INPU
KZER  ,DATA  ,1
KØNE  ,DATA  ,1
KTWØ  ,DATA  ,1
KTRE  ,DATA  ,1
KFØR  ,DATA  ,1
KFIV  ,DATA  ,1
AZER  ,DATA  ,1
AØNE  ,DATA  ,1
ATWØ  ,DATA  ,1
DIVR  ,DATA  ,100
FLAG  ,DATA  ,1
FLAX  ,DATA  ,1
SEE   ,CALL  ,FMAX
      ,JSS3  ,*+6
      ,CALL  ,DISP
      ,JMP   ,030000
      ,JMP   ,NDIS
NDIS  ,LDA   ,MAXM
      ,DAR   ,
      ,STA   ,MAXM
      ,LDX   ,=14
      ,CALL  ,INPU
      ,SUB   ,='1'
      ,JAZ   ,REP1
      ,DAR   ,
      ,JAZ   ,REP2
      ,JMP   ,NDIS
REP1  ,LDA   ,MAXM
      ,ASLA  ,4
      ,IAR   ,
      ,JMPM  ,XSQT
      ,NØP   ,
      ,NØP   ,
      ,JAZ   ,ZERØ
      ,ASRA  ,2
      ,STAE  ,STØ,1
      ,LDA   ,MAXM
      ,IAR   ,
      ,SUBE  ,STØ,1
      ,JAN   ,ZERØ
      ,JAZ   ,ZERØ
      ,STA   ,MAXM
      ,STAE  ,STØ,1
      ,DXR   ,
```

```
       ,JXZ   ,ZERØ
       ,JMP   ,REP1
REP2   ,LDA   ,MAXM
       ,ASLA  ,2
       ,IAR   ,
       ,JMPM  ,XSQT
       ,NØP   ,
       ,NØP   ,
       ,JAZ   ,ZERØ
       ,STAE  ,STØ,1
       ,LDA   ,MAXM
       ,IAR   ,
       ,SUBE  ,STØ,1
       ,JAN   ,ZERØ
       ,JAZ   ,ZERØ
       ,STA   ,MAXM
       ,STAE  ,STØ,1
       ,DXR   ,
       ,JXZ   ,ZERØ
       ,JMP   ,REP2
ZERØ   ,TZA   ,
       ,STAE  ,STØ,1
       ,JXZ   ,BEG1
       ,DXR   ,
       ,JMP   ,ZERØ
BEG1   ,LDX   ,=017700
       ,TZA   ,
       ,STA   ,MARK
       ,STA   ,MARK+1
       ,TZB   ,
       ,LDA   ,0,1
       ,STAE  ,BUF,2
       ,ADD   ,1,1
       ,ASRA  ,1
       ,IBR   ,
       ,STAE  ,BUF,2
       ,LDA   ,1,1
       ,IBR   ,
       ,STAE  ,BUF,2
       ,ADD   ,2,1
       ,ASRA  ,1
       ,IBR   ,
       ,STAE  ,BUF,2
       ,TXA   ,
       ,SUB   ,=010100
       ,JAN   ,BEG5
       ,LDA   ,0,1
       ,ADDE  ,-64,1
       ,ASRA  ,1
       ,IBR   ,
```

```
      ,STAE  ,BUF,2
      ,LDA   ,0,1
      ,ADDE  ,-64,1
      ,ADD   ,1,1
      ,ADDE  ,-63,1
      ,ASRA  ,2
      ,IBR   ,
      ,STAE  ,BUF,2
      ,LDA   ,1,1
      ,ADDE  ,-63,1
      ,ASRA  ,1
      ,IBR   ,
      ,STAE  ,BUF,2
      ,LDA   ,1,1
      ,ADD   ,2,1
      ,ADDE  ,-63,1
      ,ADDE  ,-62,1
      ,ASRA  ,2
      ,IBR   ,
      ,STAE  ,BUF,2
      ,JMP   ,BEG4
BEG5  ,TZA   ,
      ,IBR   ,
      ,STAE  ,BUF,2
      ,IBR   ,
      ,STAE  ,BUF,2
      ,IBR   ,
      ,STAE  ,BUF,2
      ,IBR   ,
      ,STAE  ,BUF,2
BEG4  ,STX   ,KEPT
      ,TZX   ,
      ,LDB   ,=14
BEG2  ,LDAE  ,BUF,1
      ,JAZ   ,*+13
      ,SUBE  ,STØ,2
      ,JAP   ,*+13
      ,DBR   ,
      ,LDAE  ,STØ,2
      ,JAZ   ,*+4
      ,JMP   ,BEG2
      ,STAE  ,BUF,1
      ,JMP   ,*+4
      ,STBE  ,BUF,1
      ,TXA   ,
      ,SUB   ,=7
      ,JAZ   ,*+5
      ,IXR   ,
      ,JMP   ,BEG2-1
      ,TZX   ,
```

```
BEG3 ,LDAE  ,BUF,1
     ,LRLA  ,4
     ,IXR   ,
     ,ØRAE  ,BUF,1
     ,LRLA  ,4
     ,IXR   ,
     ,ØRAE  ,BUF,1
     ,LRLA  ,4
     ,IXR   ,
     ,ØRAE  ,BUF,1
     ,STA   ,CHU
     ,TXA   ,
     ,SUB   ,=7
     ,JAZ   ,*+8
     ,LDA   ,MARK+1
     ,CALL  ,SENE
     ,IXR   ,
     ,JMP   ,BEG3
     ,LDA   ,MARK+1
     ,ADD   ,=32
     ,CALL  ,SENE
     ,INR   ,MARK+1
     ,INR   ,MARK
     ,LDA   ,=32
     ,SUB   ,MARK
     ,JAZ   ,*+4
     ,JMP   ,*+16
     ,STA   ,MARK
     ,LDA   ,=32
     ,ADD   ,MARK+1
     ,STA   ,MARK+1
     ,LDA   ,KEPT
     ,SUB   ,=0176
     ,STA   ,MINM
     ,LDA   ,KEPT
     ,SUB   ,=010076
     ,JAZ   ,030000
     ,LDX   ,MINM
     ,JMP   ,BEG1+4
     ,INR   ,KEPT
     ,INR   ,KEPT
     ,LDX   ,KEPT
     ,JMP   ,BEG1+4
KEPT ,DATA  ,0
     ,LDA   ,SQTS+2
     ,LDB   ,SQTS
     ,RETU  ,*
XSQT ,BES   ,0
     ,SØF   ,
     ,JAN*  ,XSQT
```

```
      ,RØF   ,
      ,INRE  ,XSQT
      ,INRE  ,XSQT
      ,JAZ*  ,XSQT
      ,STB   ,SQTS
      ,STA   ,SQTS+1
      ,ASRA  ,1
      ,STA   ,SQTS+2
      ,TZA   ,
      ,LDB   ,SQTS+1
      ,DIV   ,SQTS+2
      ,TBA   ,
      ,ADD   ,SQTS+2
      ,ASRA  ,1
      ,TAB   ,
      ,SUB   ,SQTS+2
      ,JAZ   ,XSQT-3
      ,STB   ,SQTS+2
      ,JMP   ,*-11
SQTS  ,BSS   ,3
SENE  ,ENTR  ,
      ,SEN   ,057,*+5
      ,NØP   ,
      ,JMP   ,*-3
      ,EXC   ,057
      ,ØAR   ,057
      ,EXC   ,0157
      ,ØME   ,057,CHU
      ,JMP*  ,SENE
STØ   ,BSS   ,15
MARK  ,BSS   ,2
CHU   ,BSS   ,1
BUF   ,BSS   ,8
      ,END   ,
```

APPENDIX 2

THE PROGRAM OF 64 x 64 IMAGE DISPLAY

```
CBD     ,TZA
        ,STA    ,KEEP
        ,STA    ,MARK
        ,LDX    ,=017700
        ,LDA    ,0,1
        ,LRLA   ,12
        ,STA    ,CHU
        ,LSRA   ,4
        ,ØRA    ,CHU
        ,STA    ,CHU
        ,LDA    ,1,1
        ,LRLA   ,4
        ,ADD    ,1,1
        ,ØRA    ,CHU
        ,STA    ,CHU
        ,LDA    ,KEEP
        ,CALL   ,SENE
        ,LDA    ,KEEP
        ,ADD    ,=32
        ,CALL'  ,SENE
        ,INR    ,KEEP
        ,INR    ,MARK
        ,LDA    ,=32
        ,SUB    ,MARK
        ,JAZ    ,*+4
        ,JMP    ,*+16
        ,STA    ,MARK
        ,LDA    ,=32
        ,ADD    ,KEEP
        ,STA    ,KEEP
        ,TXA
        ,SUB    ,=0176
        ,STA    ,MINM
        ,TXA
        ,SUB    ,=010076
        ,JAZ    ,030000
        ,LDX    ,MINM
        ,JMP    ,CBD+4
        ,IXR
        ,IXR
        ,JMP    ,CBD+4
SENE    ,ENTR
        ,SEN    ,057,*+5
        ,NØP
        ,JMP    ,*-3
        ,EXC    ,057
        ,ØAR    ,057
        ,EXC    ,0157
        ,ØME    ,057,CHU
        ,JMP*   ,SENE
KEEP    ,BSS    ,1
MARK    ,BSS    ,1
CHU     ,BSS    ,1
MINM    ,BSS    ,1
```

APPENDIX 3

THE PROGRAM OF M.T.F. IN BASIC

```
10   REM PRØGRAM FØR MTF AT VARIØUS FREQUENCY
20   DIM L(64)
30   INPUT P
40   FØR X= 1 TØ P
50   READ L(X)
60   PRINT L(X);
70   NEXT X
80   PRINT
90   FØR Y= 1 TØ 32
100  LET N= 2*Y/ 64
110  LET A= 0
120  LET B= 0
130  FØR X= 1 TØ P- 1
140  LET A=A+L(X)
150  LET C= 2* 3.14159*N
160  LET D=(SIN(C*X)-SIN(C*(X- 1)))/C
170  LET F=L(X)*D
180  LET B=B+F
190  NEXT X
200  LET M=B/A
210  LET N1=N* 10/ 4
220  PRINT N1,M
230  NEXT Y
240  DATA 6120, 5966, 5786, 5598, 5230, 4952, 4598, 4371, 3847
250  DATA 3443, 3101, 2815, 2391, 2039, 1766, 1488, 1233, 1132, 856
260  DATA 735, 620, 461, 398, 334, 269, 212, 174, 156, 138
270  END
```

APPENDIX 4

THE PROGRAM OF MATRIX INVERSION IN BASIC

```
10    REM SØLUTIØN ØF SIMULTANEØUS EQUATIØN
20    DIM C(6,6),D(6),E(6,6),F(6),G(6),X(6),P(6,6)
30    INPUT M
40    MATREAD C(M,M),D(M)
50    MAT E=CØN(M,M)
60    MAT F=CØN(M)
70    MAT G=CØN(M)
80    MAT X=CØN(M)
90    MAT P=CØN(M,M)
100   MAT P=C
110   PRINT "CØEFFICIENT MATRIX"
120   MATPRINT C;
130   PRINT "RIGHT HAND SIDE"
140   MATPRINT D,
150   MAT E=INV(C)
160   MAT X=E*D
170   PRINT "SØLUTIØN VECTØR"
180   MATPRINT X,
190   MAT F=P*X
200   MAT G=D-F
210   PRINT "ERRØR VECTØR"
220   MATPRINT G,
230   DATA 3711, 10323, 7095, 3548, 5033, 964, 2540, 8070, 6489
240   DATA 3947, 6221, 1527, 1759, 6394, 5769, 3796, 6973, 2110
250   DATA 960, 4145, 3831, 4247, 6480, 1740, 653, 3102, 3471, 3362
260   DATA 6770, 2738, 251, 1398, 2053, 1889, 5675, 3878
270   DATA 3711, 1484, 594, 111, 37, 0
280   END
```

REFERENCES

Aronow, S. (1973)
Performance analysis of imaging systems
Seminars in Nuclear Medicine 3:239.

Bell, R.L. and DeNardo, G.L. (1970)
Enhanced scintigraphic information display using computer-generated ratio techniques
Journal of Nuclear Medicine 11:655.

Brown, D.W. (1964)
Digital computer analysis and display of the radioisotope scan
Journal of Nuclear Medicine 5:802.

Brown, D.W., Kirch, D.L., Trow, R.S., LeFree, M.T., and Steel, P.P. (1973)
Quantification of the radionuclide image
Seminars in Nuclear Medicine 3:311.

Brown, D.W., Kirch, D.L., Trow, R.S. and LeFree, M.T. (1974)
Optical image enhancement in nuclear medicine
Biomedical Sciences Instrumentation 10:161.

Boyd, C.M., Lane, J.M., Dalrymple, G.V., Baker, M.L. and Nash, J.C. (1974)
Equipment
In Basic Science Principles of Nuclear Medicine, p 198
Edited by Boyd, C.M. and Dalrymple, G.V.
C.V. Mosby Company, St. Louis.

Cahill, P. and Lawrence, M.B. (1970)
The preliminary application of a matrix inversion method for radionuclide imaging
Journal of Nuclear Medicine 11:613.

Edwards, D.N. (1974)
Do we need a computer? A review of data processing applications in nuclear medicine and radiotherapy
Clinical Radiology 25:19.

Glass, H.I. (1973)
The role of computers in the nuclear medicine laboratories
Seminars in Nuclear Medicine 3:303.

Gustafssan, T. (1972)
Computer evaluation of scintigraphic images
Acta Radiologica Supplement (Stockholm) 313:209.

Higgins, H.P., Mergeles, J.E., Vidal, E.R. and Gomes, M. (1968)
Organ visualisation with the "Gamma Camera"
Canadian Medical Association Journal 99:214.

Hine, G.J. and Erickson, J.J. (1974)
Advances in scintigraphic instruments
In Instrumentation in Nuclear Medicine, p 1
Edited by Hine, G.J. and Sorenson, J.A.
Academic Press, New York and London.

Jahns, M.F., Garza, A.L., Haynie, T.P. (1972)
A computerized scintillation data system for the gamma camera
Computers in Biology and Medicine 2:251.

Keyes, W.I., Barber, D.C. and Mallard, J.R. (1973)
Quantitative multi-level display of radioisotope scan data via a small digital computer
Physics in Medicine and Biology 18:133.

MacIntyre, W.J. (1972)
The application of computers to functional radionuclide scanning
Japanese Journal of Nuclear Medicine 9:336.

Mamoru Nakamura, Yoshikazu Sawai, Mitsunobu Abe and Fumihiko Hoshino (1973)
Application of 4096 channel memory unit to the radionuclide imaging
Tohoku Journal of Experimental Medicine 110:69.

Mould, R.F. and Wyld, C. (1973)
A comparison between line printer and conventional Polaroid gamma camera displays using a liver phantom off-line computer and contour mapping package
Physics in Medicine and Biology 18:88.

Pizer, S.M., Brownell, G.L. and Chesler, D.A. (1974)
Scintigraphic data processing
In Instrumentation in Nuclear Medicine, p 230
Edited by Hine, G.J. and Sorenson, J.A.
Academic Press, New York and London.

Sharp, P. and Mallard, J. (1974)
A proposed model for the visual detection of signals in radioisotope display images
Physics in Medicine and Biology 19:348.

Shepars, H. and Winkler, C. (1964)
An automatic scanning system using a tape perforator and computer techniques
In Proceedings of the Symposium on Medical Radioisotope Scanning, Athens, April 20th-24th, Vienna, I.A.E.A.

Vernon, P. and Glass, H.I. (1971)
Processing gamma camera data obtained from an off-line system
In Dynamic Studies with Radioisotopes in Medicine, Vienna, I.A.E.A.